

RNI: DELENG/2005/15153

Publication: 15th of every month

Posting: 19th/20th of every month at NDPSO

No: DL(E)-01/5079/17-19

Licensed to post without pre-payment U(E) 28/2017-19

Rs.150

ISSN 0973-2136

www.mycoordinates.org

Coordinates

Volume XIII, Issue 08, August 2017

THE MONTHLY MAGAZINE ON POSITIONING, NAVIGATION AND BEYOND

***INDOOR
POSITIONING***

PGM2016: A new Geoid Model for the Philippines

Be Captivated

Visit www.leica-geosystems.com/becaptivated
to find out more and request a demonstration.

Viva

Leica Viva GS16 Experience 3D innovation

Meet the self-learning GNSS, powered by RTKplus and SmartLink and seamlessly connecting with the new Leica Captivate touch-technology software. While RTKplus automatically selects the optimal GNSS signals with a robust 555-channel engine, SmartLink uses precise point positioning technology to stay connected. Experience 3D innovation with the most accurate positions and complete the job from anywhere.



Leica Geosystems AG
leica-geosystems.com



- when it has to be **right**

Leica
Geosystems

KCS TraceME

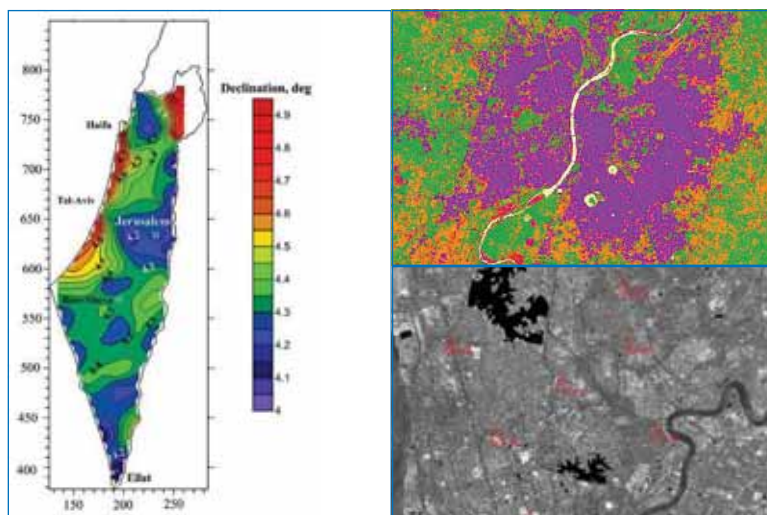


WORLDWIDE DISTRIBUTOR REQUESTS ARE WELCOME!

KCS always expands their distribution network worldwide. Please have a look at our company website for product details. We are only looking for financial strong distributors who understand our product line and programming scripts and can fully support their customers. Please feel free to send your distributor request. **For KCS TraceME / LoRa Track & Trace product requests please fill in our web form.**

www.Trace.ME

All trademarks mentioned herein belong to their respective owners.



In this issue

Coordinates Volume 13, Issue 08, August 2017

Articles

Indoor Positioning Using Probabilistic Virtual Anchor Point Graphs EIKE JENS HOFFMANN 6 **Synchronet service demonstration results in DEMETRA H2020 Project** ENRICO VARRIALE AND QUIRINO MORANTE 11 **GNSS data for ionosphere characterization** JOSIP VUKOVIC AND TOMISLAV KOS 19 **PGM2016: A new Geoid Model for the Philippines** R GATCHALIAN, R FORSBERG AND A OLESEN 31

Columns

My Coordinates EDITORIAL 6 **Old Coordinates** 18 **News** IMAGING 41 UAV 42 GIS 44 GNSS 45 GLONASS UPDATE 46 GALILEO UPDATE 22 INDUSTRY 47 **Mark your calendar** SEPTEMBER 2017 TO APRIL 2018

This issue has been made possible by the support and good wishes of the following individuals and companies

A Olesen, Eike Jens Hoffmann, Enrico Varriale, Josip Vuković, Quirino Morante, R.Gatchalian, R Forsberg and Tomislav Kos and; Effigis, HiTarget, IP Solutions, Javad, Leica, Pentax, SBG Systems, Spectra, Trace Me and many others.

Mailing Address

A 002, Mansara Apartments
C 9, Vasundhara Enclave
Delhi 110 096, India.
Phones +91 11 42153861, 98102 33422, 98107 24567

Email

[information] talktous@mycoordinates.org
[editorial] bal@mycoordinates.org
[advertising] sam@mycoordinates.org
[subscriptions] iwant@mycoordinates.org

Web www.mycoordinates.org

Coordinates is an initiative of CMPL that aims to broaden the scope of positioning, navigation and related technologies. CMPL does not necessarily subscribe to the views expressed by the authors in this magazine and may not be held liable for any losses caused directly or indirectly due to the information provided herein. © CMPL, 2017. Reprinting with permission is encouraged; contact the editor for details.

Annual subscription (12 issues)
[India] Rs.1,800 [Overseas] US\$100

Printed and published by Sanjay Malaviya on behalf of Coordinates Media Pvt Ltd

Published at A 002 Mansara Apartments, Vasundhara Enclave, Delhi 110096, India.

Printed at Thomson Press (India) Ltd, Mathura Road, Faridabad, India

Editor Bal Krishna

Owner Coordinates Media Pvt Ltd (CMPL)

This issue of Coordinates is of 52 pages, including cover.



Artificial Wisdom

Elon Musk, the chief of Tesla and SpaceX

Has repeatedly been admonishing

On potentially apocalyptic future of Artificial Intelligence (AI)

and appealing for proactive regulations on AI.

However, Mark Zuckerberg, Facebook's CEO

Has called Musk a 'naysayer'

And termed his doomsday prophecy as result of unnecessarily negativity.

If the increasing obsession of mankind with AI,

Could be evolved towards

Artificial Wisdom,

The 'killer robots' may turn into the 'savior ones'.

However, the dependence on 'the artificial'

Will continue to question

The 'wisdom' of 'human intelligence'.

Bal Krishna, Editor
bal@mycoordinates.org

ADVISORS Naser El-Sheimy PEng, CRC Professor, Department of Geomatics Engineering, The University of Calgary Canada, George Cho Professor in GIS and the Law, University of Canberra, Australia, Professor Abbas Rajabifard Director, Centre for SDI and Land Administration, University of Melbourne, Australia, Luiz Paulo Souto Fortes PhD Associate Professor, University of State of Rio Janeiro (UERJ), Brazil, John Hannah Professor, School of Surveying, University of Otago, New Zealand

Indoor Positioning using probabilistic Virtual Anchor Point graphs

Hybrid indoor positioning with concept of Virtual Anchor Points along with Bluetooth Low Energy tags saves infrastructure and maintenance costs



Eike Jens Hoffmann
Mobile and Distributed
Systems Group
LMU Munich, Germany

Along with the evolution of mobile devices a wide landscape of applications tailored for mobile usage has been developed. To make them as smart as possible most of them take the user's current context into account, amongst others time and location. While location in outdoor environments can be easily obtained from GPS sensors, in indoor scenarios this is not possible due to shielding and scattering of GPS signals.

Enabling indoor positioning has been a large research field during the last years with approaches relying on dead reckoning, Bluetooth, and Wi-Fi signals. Especially the last technology gained a lot of attention since Wi-Fi fingerprinting solutions turned out to be among the most accurate ones [1].

Additionally, after releasing the Bluetooth Low Energy (BLE) standard a new class of devices was unveiled: the so-called BLE beacons or tags. Once deployed at a fixed position they provide a proximity interface for positioning, dividing distance into discrete factors like *far*, *near* and *immediate*.

In our concept called Virtual Anchor Points (VAP) [2], we demonstrated how unambiguous patterns of receivable Wi-Fi fingerprints can be extracted from time-series of Wi-Fi readings. Furthermore, these patterns can be used to form virtual beacons providing a proximity interface analogous to BLE tags. That is why we called our concept Virtual Anchor Points.

In this paper we extend the existing proximity detection algorithm using a simple next neighbor classifier with a

solution called graph particle filter. In the next section, we provide an overview over the related work and show the differences to our system. Next, in the third Section we give a short explanation of the VAP concept and describe how this concept can be extended with a particle filter. Afterwards we evaluate the graph particle filter comprehensively against our existing approach and conclude the results in the last section.

Related work

The research field for indoor positioning using Wi-Fi infrastructure is comprehensive: one of the first solutions was RADAR [3] a radio-frequency (RF based on next neighbor matching of fingerprints. Further improvements to Wi-Fi fingerprinting were introduced by using probabilistic frameworks [4], [5] and sensor fusion combining IMU data and Wi-Fi data in particle filtering methods [6]–[9].

In this paper we extend the simple next neighbor proximity detection method used in the online phase of the Virtual Anchor Points concept with a new one called graph particle filtering, which solely relies on time and Wi-Fi data without incorporating further sensor data.

Method

In this section we first describe briefly how Virtual Anchor Points are extracted from Wi-Fi time series data during the offline phase and present the existing proximity detection based on a next neighbor

Existing approach for proximity detection of Virtual Anchor Points relies on simple next neighbor classifier

classifier as well as the new graph particle filter detection for online usage.

Creating Virtual Anchor Points

We use Wi-Fi time series as input data in which each timestamp is associated with a set of Basic Service Set Identifications (BSSID) b and their respective Received Signal Strength Indications (RSSI) r from access points (AP) within reach $(t, \{(b_0, r_0), \dots, (b_m, r_m)\})$, $m \in \mathbb{N}$. Based on this time series data VAPs are created with three steps: first, candidates for anchor points are extracted from the time series data. Next, these candidates are projected into a lower dimensional space using multidimensional scaling. Within this space, unambiguous candidates can be filtered out from ambiguous ones, resulting in a final set of VAPs.

We assume that our time series data carry annotations about the places visited during recording, which can be used for the extraction of candidates. Using a time window of five seconds around an annotation we calculate the mean RSSI and its standard deviation for each measured BSSID. Thus, for each annotation we have a set of quadruples (b, μ, σ, n) with b denoting the BSSID, μ and σ describing a normal distribution using mean, and standard deviation and denoting the number of measurements for b in the time window. Sets of quadruples with the same annotation are merged with the portioning algorithm from Chan et al. [10] to a candidate $C = \{(b, \mu, \sigma, n)_0, \dots, (b, \mu, \sigma, n)_m\}$, $m \in \mathbb{N}$. All candidates are collected in the final candidate set \mathcal{C} .

To be brief, the next step sets up a dissimilarity matrix for multidimensional scaling to project all candidates into a lower dimensional Euclidean space. In this space we express uniqueness by the standard deviation of the measurements taken. Therefore, we first compute the mean standard deviation of each candidate $C \in \mathcal{C}$:

$$\bar{\sigma}_C = \frac{1}{|C|} \sum_{(b, \mu, \sigma, n) \in C} \sigma$$

Next, we have to scale this value into

the model space, thus we calculate the mean ratio between pairwise distances in model space d_{mds} and signal space d_{sig} :

$$\tau = \frac{1}{|\mathcal{C}|^2} \sum_{g \in \mathcal{C}} \sum_{h \in \mathcal{C}} \frac{d_{mds}(g, h)}{d_{sig}(g, h)}$$

Since the mapping using τ is very coarse we add an additional scaling parameter ρ and define a sphere distance $d_{sph}(g, h) = d_{mds}(g, h) - \rho \cdot \tau \cdot (\bar{\sigma}_g - \bar{\sigma}_h)$ to check if two candidates intersect in the Euclidean space. Thus, we can now define a VAP as a candidate, which does not overlap with other candidates:

$$g \in \mathcal{C} \text{ is VAP} \Leftrightarrow \forall h \in \mathcal{C}, h \neq g : d_{sph}(g, h) \geq 0$$

By filtering out intersecting candidates from based on we obtain a set of VAPs denoted as \mathfrak{V}_ρ .

Proximity detection using next neighbor classifier

For online usage we compare the observed Wi-Fi access points and their RSSI denoted as measurement $z_t = \{(b_z, r_z)_j\}$ to all VAPs \mathfrak{V}_ρ using a next neighbor classifier:

$$\operatorname{argmin}_{v \in \mathfrak{V}} \{d(v, z_t)\}$$

Since RSSI varies highly over time even at the same place [11]–[13] we implemented a first in first out (fifo) queue with fixed size to keep track of the last n measurements (Figure 1). This queue supports two different operations: first, returning the union set of all seen BSSIDs and second, returning the intersection set of all BSSIDs, both with their respective mean RSSIs. Thus, querying the queue results in an aggregated measurement \hat{z}_t ,

combining multiple single measurements z .

Proximity detection using graph particle filter

Since all VAPs have their origin in time series, the previous and next VAPs can be easily derived from this data. Thus, we are able to connect all VAPs in a graph $G=(V, E)$ with each VAP as a vertex $v \in V$ and edges $e \in E$ denoting if two VAPs are next to each other and labeled with the time it takes to walk from one VAP to another.

Our existing approach for detecting the next VAP is based on simple next neighbor algorithm, which calculates the distance from the currently observed fingerprint and all VAPs and returns the VAP with the lowest distance. However, this approach does not take previous proximity detections into account, which can be helpful if RSSIs have a large variance. To make our novel method more robust and less dependent on single measurements we implemented a particle filter on this graph.

Particle filters implement a recursive Bayesian filter based on the sequential Monte-Carlo method [14] By using a set of random samples $\{x_t^i, i = 1, \dots, N\}$ that are called particles the filter estimates the probability density function of the state x_t at time t :

$$p(x_t | z_t) \approx \sum_{i=1}^N w_t^i \delta(x_t - x_t^i)$$

with z_t as a measurement at time t , w_t^i as the weight of particle x_t^i and δ as a distance function.

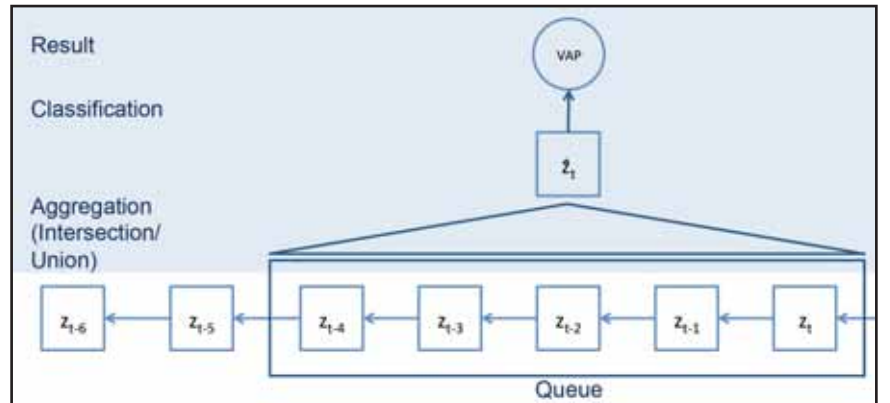


Figure 1: First in first out queue for aggregating five measurements

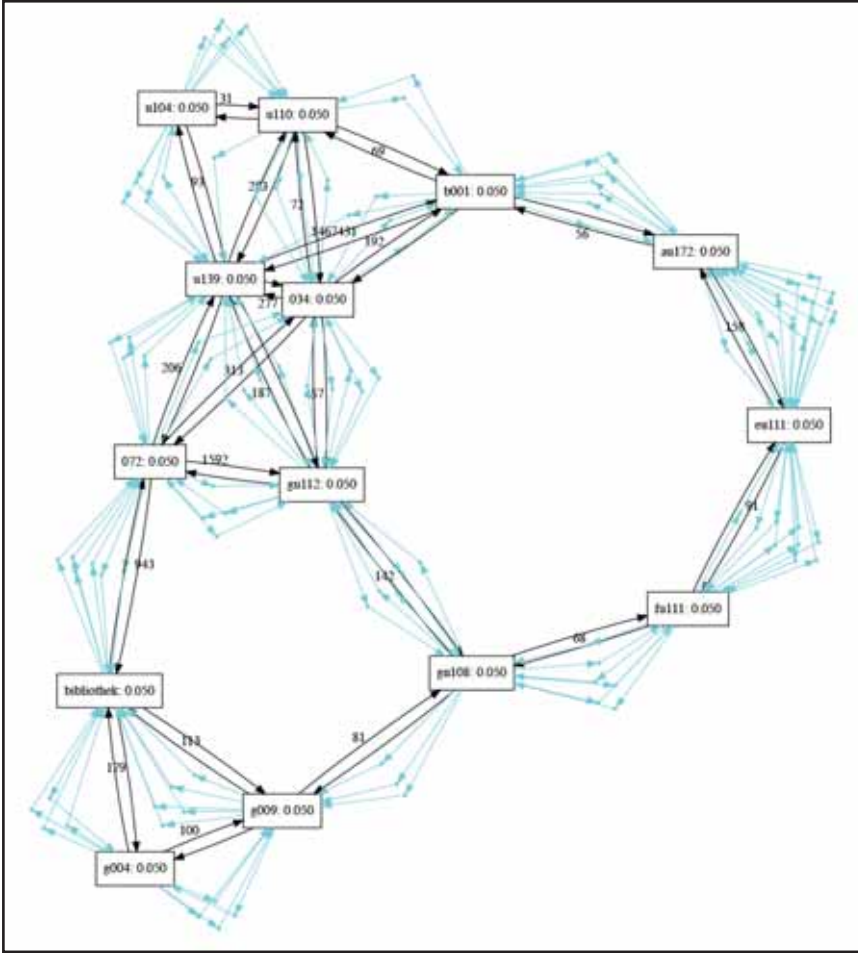


Figure 2: Example of a graph particle filter state after initialization with VAPs as vertices, black edges showing neighbor relations, and blue points as particles on the edges

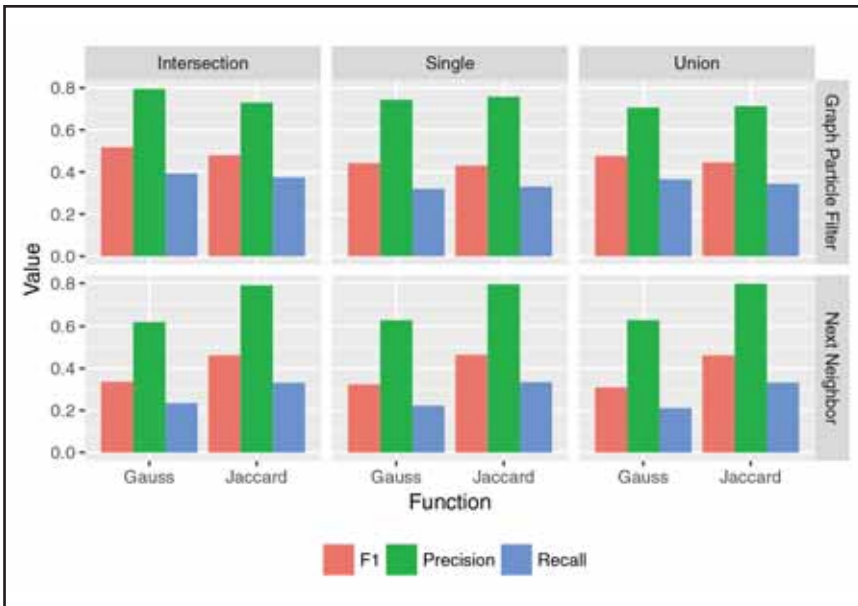


Figure 3: Precision, recall, and F1-measure for both proximity detection methods, graph particle filter and next neighbor classifier, evaluated with different smoothing and probability functions

In our case particles travel along edges based on the time between two measurements and are weighted according to the probability that the current measurement is observed next to a VAP.

$$w_t^i = w_{t-1}^i \cdot p(z_t | x_t^i)$$

The next VAP for a particle is calculated as follows. Let $e = (v_1, v_2, t_e)$ be the edge between two VAPs v_1, v_2 with a distance t_e denoting the time it takes to get from v_1 to v_2 . Since each particle has a time t_x that it spends on the edge, we can calculate the next VAP v_x for a particle x_t^i as follows:

$$v_x = \begin{cases} v_1 & \text{if } t_x < \frac{t_e}{2} \\ v_2 & \text{otherwise} \end{cases}$$

The probability of a measurement $z_t = \{(b_z, r_z)_j\}$ as a set of tuples of BSSIDs and RSSIs observed next to a VAP $v_x = \{(b_x, \mu_x, \sigma_x, n_x)_k\}$ can be calculated in two ways: either with a Gauss Kernel [4] or with the Jaccard index [2] interpreted as a probability. The Gauss Kernel probability $p(z_t | x_t^i)$ is calculated based on the set I of BSSIDs in common:

$$I = \{b, b \in z_t \wedge b \in v_x\}$$

$$p(z_t | x_t^i) = \frac{1}{|I|} \sum_{b \in I} K((b_z, r_z), (b_x, \mu_x, \sigma_x, n_x))$$

$$K((b_z, r_z), (b_x, \mu_x, \sigma_x, n_x)) = \frac{1}{\sqrt{2\pi}\sigma_x} \exp\left(-\frac{(r_z - \mu_x)^2}{\sigma_x}\right)$$

The Jaccard index is RSSI agnostic because it only compares present and absent BSSIDs in both sets:

$$p(z_t | x_t^i) = \frac{I}{|z_t| + |v_x| - I}$$

Furthermore, the fifo-queue described above can be applied to the graph particle filter as well to obtain a more stable and reliable measurement.

Figure 2 shows an example how particles are distributed equally on all edges of the graph after initialization. Blue points symbolize the particles on the edges with their heading depicted in the arcs. Since the graph is directed, but edges can be traversed in both directions, there is an edge for each direction, labeled with the time it takes to walk from one VAP to another. At this state, each VAP has an equal probability of being the next anchor point, which is indicated by the value behind the label.

Evaluation

In this section, we show how the graph particle filter approach performs against the existing next neighbor classifier. To make the particle filter results comparable with the next neighbor approach, we concentrated on VAP vertices in the graph with at least one neighbor. Thus, we adapted our test dataset [2] as well and evaluated on 6,203 fingerprints containing RSSIs from 242 different BSSIDs.

Figure 3 depicts how both proximity detection algorithms behave with different aggregation methods and different probability functions. In all experiments the precision is about two times higher than the recall with a precision mean value of 0.73 versus a recall mean value of 0.32. Given a new measurement a high precision is desirable for predicting the next VAP.

Generally speaking, the graph particle filter performs 6 % better using a Gauss kernel than the Jaccard index with respect to the F1-measure. In contrast the next neighbor

classifier works best with the Jaccard index, which is a 43 % improvement in F1-measure over a Gauss kernel.

If we take a closer look at the interaction between aggregation methods and probability functions, differences get more obvious. As already stated in our previous work, the next neighbor classifier works best with the Jaccard index in combination with the union set aggregation method. This combination leads to a precision of 0.80, a recall of 0.33, and an overall F1-measure of 0.46. The graph particle filter has its best performance after aggregating using the intersection method and comparing the measurement with the Virtual Anchor Points using a Gauss kernel. Here, we have a precision of 0.80, a recall of 0.39, and an overall F1-measure of 0.51.

Thus, with respect to precision, both methods perform equally, but recall is 18 % higher when using the graph particle filter instead of the next neighbor classifier. In the end, the graph particle

Experiment results

show a 12 % better F1-measure of graph particle filter compared to next neighbor classifier

filter has 12 % higher F1-measure than the next neighbor classifier.

Both methods behave completely different when using the same aggregation and probability functions. The graph particle filter works best with the Gauss kernel and an aggregation based on the intersection set of all observed access points. Both parts are closely related because the Gauss kernel takes the RSSIs into account and by focusing on the BSSIDs, which were observed in all measurements of the fifo-queue, their RSSI values become stable. Additionally, the graph particle filter takes the previous state



REAL-TIME SIMULATION

GPS / GLONASS / BEIDOU
GALILEO / QZSS / SBAS

EXTENSIVE MODELLING SUITE
IONOSPHERIC SCINTILLATION

GNSS TECHNOLOGY SINCE 2007

WWW.IP-SOLUTIONS.JP **SALES: KYRON@IP-SOLUTIONS.JP**

into account and allows no jumps in the graph, leading to a further stabilization of all predictions. In contrast to this, the next neighbor classifier performs best when using the Jaccard index, which is completely RSSI agnostic. Since it only compares the present and absent BSSIDs, the union set of all measurements provides more information about the APs within reach. For a prediction that has no information about the past this approach combines the most information without relying on unstable RSSI data.

Conclusion


In this paper we extended our existing concept of VAPs and their proximity detection with a novel approach that we call graph particle filter. In contrast to other methods that use sensor fusion, our particle filter takes only time and Wi-Fi readings for predicting the next VAP. Using this filter we could improve the proximity detection compared to the existing next neighbor classifier by 12 % (F1-measure) and gain an overall precision of 80 %.

Our graph particle filter is not limited to VAP but can also include BLE tags as nodes, leading to a hybrid framework that can serve as an abstraction layer over physical tags and VAPs.

In future work, we want to extend this set of VAPs with points in signal space, which are sufficiently distinguishable from the current set of VAPs and which have a sufficient support in the time series set in the sense that enough people have observed these places. These points

could then be pushed out to the service asking users to assign labels to them.

References

- [1] H. Liu, H. Darabi, P. Banerjee, and J. Liu, "Survey of Wireless Indoor Positioning Techniques and Systems," *IEEE Trans. Syst. Man Cybern. Part C (Applications Rev.)*, vol. 37, no. 6, pp. 1067–1080, Nov. 2007.
- [2] E. J. Hoffmann, M. Werner, and L. Schauer, "Indoor navigation using virtual anchor points," in *2016 European Navigation Conference, ENC 2016*, 2016.
- [3] P. Bahl and V. N. Padmanabhan, "RADAR: an in-building RF-based user location and tracking system," in *Proceedings IEEE INFOCOM 2000. Conference on Computer Communications. Nineteenth Annual Joint Conference of the IEEE Computer and Communications Societies (Cat. No.00CH37064)*, 2000, vol. 2, pp. 775–784.
- [4] T. Roos, P. Myllymäki, H. Tirri, P. Misikangas, and J. Sievänen, "A Probabilistic Approach to WLAN User Location Estimation," *Int. J. Wirel. Inf. Networks*, vol. 9, no. 3, pp. 155–164, 2002.
- [5] M. Youssef and A. Agrawala, "The Horus WLAN location determination system," in *Proceedings of the 3rd international conference on Mobile systems, applications, and services - MobiSys '05*, 2005, p. 205.
- [6] J. Seitz, T. Vaupel, and J. Thielecke, "A particle filter for Wi-Fi azimuth and position tracking with pedestrian dead reckoning," in *2013 Workshop on Sensor Data Fusion: Trends, Solutions, Applications (SDF)*, 2013, pp. 1–6.
- [7] M. M. Atia, M. J. Korenberg, and A. Noureldin, "Particle-Filter-Based Wi-Fi-Aided Reduced Inertial Sensors Navigation System for Indoor and GPS-Denied Environments," *Int. J. Navig. Obs.*, vol. 2012, pp. 1–12, Jun. 2012.
- [8] N. Zhu, H. Zhao, W. Feng, and Z. Wang, "A novel particle filter approach for indoor positioning by fusing WiFi and inertial sensors," *Chinese J. Aeronaut.*, vol. 28, no. 6, pp. 1725–1734, Dec. 2015.
- [9] Z. Wu, E. Jedari, R. Muscedere, and R. Rashidzadeh, "Improved particle filter based on WLAN RSSI fingerprinting and smart sensors for indoor localization," *Comput. Commun.*, vol. 83, pp. 64–71, 2016.
- [10] T. F. Chan, G. H. Golub, and R. J. LeVeque, "Updating formulae and a pairwise algorithm for computing sample variances," in *COMPSTAT 1982 5th Symposium held at Toulouse 1982*, 1982, pp. 30–41.
- [11] K. Kaemarungsi and P. Krishnamurthy, "Properties of indoor received signal strength for WLAN location fingerprinting," in *Proceedings of MOBIQUITOUS 2004 - 1st Annual International Conference on Mobile and Ubiquitous Systems: Networking and Services*, 2004, pp. 14–23.
- [12] M. Kranz, C. Fischer, and A. Schmidt, "A comparative study of DECT and WLAN signals for indoor localization," in *2010 IEEE International Conference on Pervasive Computing and Communications (PerCom)*, 2010, pp. 235–243.
- [13] K. Kaemarungsi and P. Krishnamurthy, "Analysis of WLAN's received signal strength indication for indoor location fingerprinting," *Pervasive Mob. Comput.*, vol. 8, no. 2, pp. 292–316, Apr. 2012.
- [14] M. S. Arulampalam, S. Maskell, N. Gordon, and T. Clapp, "A tutorial on particle filters for online nonlinear/non-Gaussian Bayesian tracking," *IEEE Trans. Signal Process.*, vol. 50, no. 2, pp. 174–188, 2002. 

Graph particle filter as improvement over next neighbor classifier uses solely time and Wi-Fi measurements for an improved localization

SYNCHRONET service demonstration results in DEMETRA H2020 project

A scalable high performances synchronisation solution



Enrico Varriale
Responsible for Timing Reference area, Thales Computer Science Specialist, Thales Alenia Space Italia, Italy



Quirino Morante
Head, GNSS SIW and Developments Unit, Domain Observation and Navigation of Thales Alenia Space Italia

SynchroNet is a Thales Alenia Space Italia patented solution for a high performance, scalable and resilient time and frequency transfer system.

The SynchroNet system addresses an arbitrarily large and topologically distributed network of nodes equipped with atomic clock(s) (ranging from inexpensive rubidium to high end oscillators like Active Hydrogen Maser) with baselines up to thousands of kilometers between any two nodes.

SynchroNet uses GNSS (Global Navigation Satellite Systems) Signal in Space to implement a distributed approach of classical time transfer and complements this function with autonomous steering functions implemented at each node to cope with Signal in Space interruptions/disruptions.

SynchroNet provides a complete set of service oriented functionalities around the core synchronisation capability, for this reason it can be suitable for a large range of application domains where synchronisation is required either in terms of accuracy or in terms of scalability or both.

This paper will provide an overview of SynchroNet architecture and capabilities as well as its declination to the DEMETRA project and the demonstration campaign results of the core synchronization capabilities as verified by the DEMETRA Service Monitoring.

DEMETRA (DEMonstrator of EGNSS services based on Time Reference

Architecture) project is funded by the European Union in the frame of the Horizon 2020 program, aimed at developing and experimenting time dissemination services based on the European GNSS. DEMETRA project has received funding from the European GNSS Agency under the European Union's Horizon 2020 research.

Introduction

Time is a recognized fundamental function of several systems, including critical ones, and all system requiring this function implement their own solution to solve this common problem. The idea of SynchroNet is born with objective to offer industry oriented solution for the provision of time thus treating time like all other fundamental services like power/energy or communication. Like the other services, the goal of an industry oriented time service provision solution is to offer a standardized "plug" used to retrieve time/synchronization information. For time to be treated as a service and for a solution to be considered industry oriented it requires that a set of some high level requirements are met, here follows a selection that driven the design of the SynchroNet solution:

- Concept of user and Time provider shall be defined
- Service provider and service products shall be traceable, integer, reserved and authentic
- Time Service shall be integrated and not designed for the user systems
- Time source interface shall be the same at any user location

- Time service performances shall be defined by a set of Service Level Agreements (SLA) that may be different for each user and for each user's site
- Each user shall be able to dimension its SLA and to control and be responsible for the service infrastructure integrated in their systems
- SLA shall be monitored and faults shall be timely reported to users
- Service shall be maintainable
- Users shall be independent and not affected by faults caused by of occurring to other users
- It shall not require timing and synchronization specialist competencies in order to be used effectively

SynchroNet is the Thales Alenia Space Italy proposed solution covering the above defined needs and providing to each user a self-contained, robust and independent reference time scale and synchronization system for each facility or unit/equipment deployed at user's premises.

SynchroNet Architecture

The general operational concept is quite simple: it is defined a stable reference time source that can be external (e.g. a UTC timing laboratory) or internal (user's own atomic time scale or provided as part of SynchroNet solution) with respect to user's infrastructures; one or more remote sites retrieve reference frequency and time from the central node or from other nodes (multi-hop hierarchical time distribution).

This concept is represented in Figure 1:

Figure 1 shows also the relevant architecture and interfaces of SynchroNet.

Three types of node are defined:

- MRT's (main reference Times): represent a time and frequency source for other nodes in the network. The reference of the whole SynchroNet network is called MRT0.
- SyN (SynchroNet leaf Node):

are nodes that simply receive synchronization results from their reference MRT

- -Control Node: controls the network topology (add, remove and logically move nodes –e.g. assign a SyN to an MRT). Also the Control Node is the root for encryption and in particular for PKI used by SynchroNet nodes.
- GNSS: SynchroNet uses GNSS signals as carriers for its internal time transfer algorithms. This means that SynchroNet is independent of the specific time distributed through Galileo or GPS (i.e. in case a time jump is introduced in any of the GPS or Galileo constellations the SynchroNet network is not affected and doesn't observe any jump, see DEMETRA stress test results)
- Communication: this is some means used to transfer digital data between each node and MRT and Control Node. Each SynchroNet node establishes two and only two point-to-point encrypted tunnels: one with MRT and one with Control Node. The two channels are independent (with separated PKI) and cannot be used to route information across the network. This architecture offers several advantages in terms

of security and easiness of network topology management but also in terms of required bandwidth at each node thus allowing to exploit also low throughput communication means to reach remote nodes (i.e. few hundreds of bits per second)

Both MRT and SyN deliver locally a physical realization of system time and frequency that can be exploited by real HW of other sub-systems. In particular, as a minimum, each node of the network (with the exclusion of Control Nodes) distributes:

- 10MHz frequency reference
- 1PulsePerSecond TTL
- NTP

Considering the nature of timing products, when designing SynchroNet some further requirements have been identified as distinctive and characterizing of the proposed solution: scalability and flexibility.

These have been captured by the following features of SynchroNet:

- It is possible to promote a SyN into an MRT at runtime without service interruption or degradation
- It is possible to move a SyN or an MRT (with all its dependency) to another MRT (e.g. in case of failure

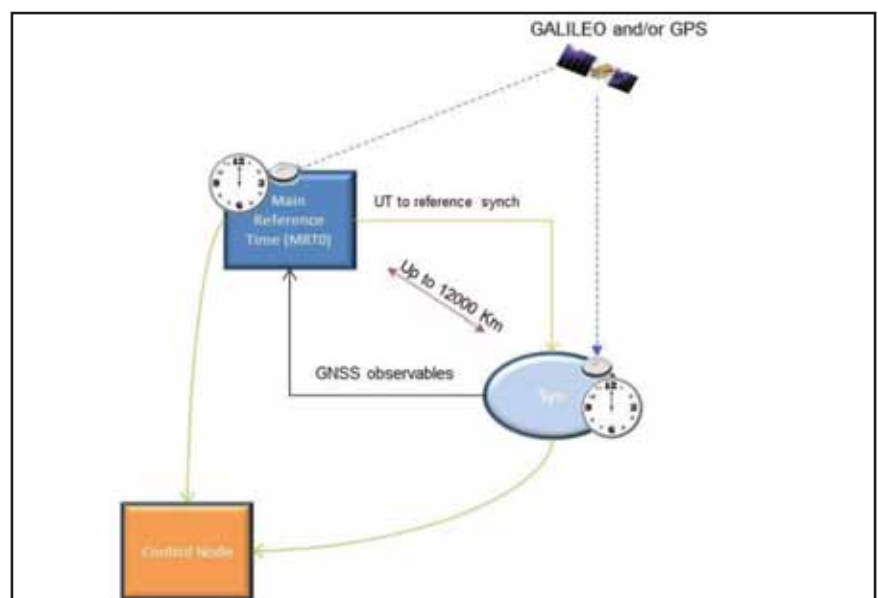


Figure 1: SynchroNet hierarchical network organisation

- or HW malfunction) at run time and without service interruptions
- It is possible to add or remove a node at run time without affecting the overall system operations
- SynchroNet nodes can be deployed with local oscillator characteristics and performances but running the same distributed solution. This means it is possible at any time to upgrade or downgrade a SynchroNet node without requiring modification in terms of system architecture or implementation.

The entire above mentioned network layout management operations can be carried out at run-time and without interruption of locally distributed timing references.

SynchroNet system also takes care of managing all low level security infrastructures for channels impacted by the reconfiguration of the network.

These features allow users to build and manage dynamically complex hierarchies.

Security

In SynchroNet security has been designed to protect two main assets:

- GNSS signals received from space
- Data exchange between any two nodes of the network

These assets are quite different in nature and with different impacts on overall system performances and availability.

GNSS threats are related to availability and authenticity which can be impaired respectively by intentional and unintentional jamming/attenuation and spoofing; an example of unintentional spoofing may be considered what happened in early 2016 to GPS in which due to an operation issue a jump in GPST has been introduced and propagated to user level.

SynchroNet exploits both the georeferenced network of nodes and internal steering algorithms to detect potential spoofing and to mitigate the effects of spoofing and jamming in terms of nodes synchronization accuracy and synchronization stability. To maximize their effectiveness, detection and mitigation are two independent processes i.e. mitigation algorithms work continuously (embedded in clock steering algorithm) also in case detection process doesn't detect any spoofing of even in case it is not working at all.

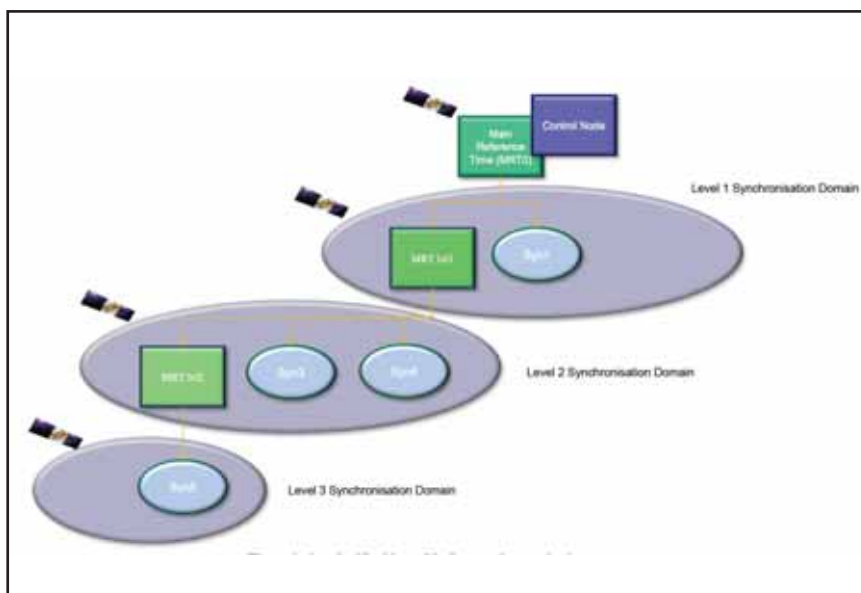


Figure 2: SynchroNet hierarchical network organisation

HI-TARGET



V90 Plus

High-end RTK receiver with multi technology integrated



BD970 GNSS engine



Support GPS, GLONASS, BDS, GALLILEO



Tilt sensor and electronic bubble integrated



NFC and WiFi functionality

BERLIN 2017 INTERGEO
26 - 28 SEPTEMBER

HI-TARGET Hall 1.1, C1.061

www.hi-target.com.cn | info@hi-target.com.cn

Data exchange between network nodes is necessary to exchange GNSS observation data, to implement monitoring and configuration and to deliver synchronization products.

In designing SynchroNet it has been decided to rely only on the assumption that nodes speak each other using IP stack thus neglecting any assumption actual channels used to deliver packets (in the same network some node may need to use cell data communication or sitcom systems, wired telephone lines, etc). This means that security measures for protecting nodes communication network operate only at Networking layer and above.

SynchroNet implements, at each node, a stacked approach aiming at ensuring authenticity, integrity and secrecy of the messages exchanged. In particular all network packets exchanged between any two nodes is carried out via a dedicated VPN whose based on a public key infrastructure, also all application level information are signed and encrypted using asymmetric encryption.

All communication channels and all levels of security uses a dedicated set of keys and signatures that are managed

by the management system coherently with the underlying logical network topology. A byproduct of this organization is that, at each node, is available an NTP service that was never exposed to external networks, whose content has been authenticated and encrypted (at the cost of some performance loss due to the asymmetry introduced by auth verification and decryption) and that is always guaranteed to be aligned to master system time (SynchroNet can operate using a custom time reference frame other than standard UTC and NTP can be configured to distribute such reference).

Network layout

SynchroNet network is inherently oriented towards a hierarchical organization that, starting from the simple layout of Figure 1, can be scaled up to cover a larger service area or an increased number of terminal keeping balanced the overall service load.

Hierarchical organization, together with flexible and run time network logical topology management, also allows to organize nodes based on their timing HW capabilities (as a rule of thumb each node should be synchronized to a node equipped with higher performance oscillators).

From layout represented in Figure 1 a SynchroNet network can scale to configurations similar to the one represented in Figure 2

A dedicated network management and configuration mechanism has been designed in order to implement scalability and flexibility oriented runtime features described in Chapter II, in order to keep manageable and effective security mechanisms and to not bound scalability to the available network and computing resources.

The solution adopted guarantees that all communications are point-to-point over two independent communication channels described in Chapter II (synchronization and M&C); the immediate benefit of

this design is that any network .logical layout modification (add, remove, assign, promote, see Chapter II) impacts at most four nodes regardless of global network size. This fact makes feasible to manage automatically security mechanisms in response to a change in network logical layout.

In particular, whatever transformation is applied to the network, the channel with Control Node is never affected, and nodes receive certificates only through this channel for which Control Node operates as Certification Authority, thus all transfer of certificates happen on point-to-point channels between each of the affected nodes and Control Node. In case a new node is deployed the keys for establishing a secure connection with Control Node are pre-installed as well as all relevant PKI and CA information.

Service performances

Since SynchroNet is a time service oriented solution the concept of service performance is tightly bounded to design and implementation decisions and in particular for what concerns monitoring capabilities and alerting.

Of course SynchroNet capabilities are defined not only in terms of synchronization accuracy and stability but also in terms of several other parameters and in particular in terms of:

- Service availability:
 - Robustness and independence from GPS or Galileo Time. This is guaranteed by relying on GNSS signals only as carriers used by time transfer algorithms.
 - Resilience to faults/ impairments of GNSS
 - Resilience to faults/impairments of communication channels
- Service configurability and maintainability
- Synchronisation performance and integrity monitoring
 - Stability
 - Accuracy
 - Uncertainty



Figure 3: SYN node prototype for use in DEMETRA

In particular for what concerns Synchronisation performance and integrity a SLA can be defined, re-defined and monitored independently for each node of the network; SLA parameter definition is achieved through a preliminary factory calibration and can be refined with monitoring results obtained during a longer operational observation period.

Also for all synchronization SLA information it is provided a double confirmation approach in which the parameters are computed and reported (locally, to Control Node and to MRT) from the node being synchronized and as well computed and reported (locally and to Control Node) by the MRT synchronizing that node.

Test campaign results

In the frame of H2020 European Community program, Thales Alenia Space Italia is participating to the DEMETRA project with a specifically adapted SynchroNet demonstrator.

DEMETRA is carried out by a consortium of national metrology institutes, university, industries and is conceived as demonstrator of different timing services devoted to different markets and user needs.

SynchroNet takes part to the DEMETRA test campaigns and is identified as Time Service#9.

DEMETRA provides to time services a common time reference frame (Italian UTC as realized at Italian Metrological Institute - INRIM) as well as a Core Infrastructure that includes a facility for independent services performance assessment and continuous monitoring managed by Italian Metrological Institute personnel.

DEMETRA Test Campaign are designed to test services and their performances both in nominal and extreme conditions considering the peculiarities of each service.

In particular for SynchroNet the following relevant test cases were defined:

- Evaluation of accuracy and stability of time transfer between MRT and SYN nodes in nominal conditions.
- Stress tests:
 - Evaluation of accuracy and continuity under strong attenuation of GNSS signals (16dB attenuation at GNSS receiver antenna)
 - Evaluation of accuracy and continuity in case of synchronization service (e.g. in case SYN is unable to talk to MRT or due to lack of GNSS signals on MRT and/or SYN)
- Evaluation of continuity and availability

For all test cases the 1PPS output of the SYN under test has been continuously monitored by DEMETRA performance monitoring facility and then compared and validated with results computed internally by SynchroNet as part of its -integrity and performance self-monitoring. Also GNSS receivers (including antenna and antenna cable) employed by SynchroNet prototype have been externally calibrated with total residual uncertainty below 3ns.

For testing purpose it has been deployed a SynchroNet SYN with minimal HW capabilities and in particular equipped with an inexpensive Rubidium oscillator as internal frequency reference.

The UT prototype is shown in Figure 3, the size is not representative of the final product since prototype rack layout was selected for reusability and easy access during further experimentation with different type of oscillators and steering equipment.

Preliminary calibration of SYN under test defined the following nominal condition SLA parameters:

- Time offset vs UTC(IT): $\leq 50\text{ns}$ (2sigma)
- Synchronisation stability @12h: 4.0e-13
- Synchronisation stability @24h: 3.0e-13



HI-TARGET

HiScan-S

Integrated
high-accuracy mobile
mapping system



High-density,
high-accuracy
point cloud



Fully matched point
cloud and panorama
images



Fully integrated
solution

BERLIN 2017 INTERGEO

26 - 28 SEPTEMBER

HI-TARGET Hall 1.1, C1.061

www.hi-target.com.cn | info@hi-target.com.cn

Here below are reported some representative results related to mentioned test cases, all results have been cross-checked with results provided by DEMETRA performance monitoring facility.

Overall performances

Instead of presenting the best achieved performances it is considered interesting to report the behavior of the SYN across the whole experimentation campaign up to the time of gathering data presented below. The overall period covered is more than 200 days during which SynchroNet prototype operated completely unmanned and without need for manual intervention or parameters fine tuning, the plots reported include of course the period in which the planned stress tests have been carried out as well as unintentional stress tests caused by networking impairments happened at DEMETRA hosting site and that caused a substantial degradation of communication capabilities between SYN and MRT for more than 21 days during which only 50% of planned synchronization took place successfully; this period is the rightmost part of the phase plots shown below.

From data series represented in Figure 4 the statistical data are derived (Table 1).

And plot reports synchronization stability in which all the instability contribution has been assumed on the SYN side (Figure 5).

Stress tests performances

Here below is reported an annotated plot of the period in which planned stress test case have been excersiced, in particular the first block (reading from left) is related to a general unavailability scenario in which in turn MRT and SYN has been disabled GNSS observable collection thus synchronization was inhibited and signal was autonomously steered by the SYN internal algorithms.

The second block of stress test has been applied after a short period used to observe autonomous recovery

	Treshold					
	10ns	20ns	30ns	40ns	50ns	60ns
% below threshold	80,73%	97,91%	99,59%	99,88%	99,98%	100%

Table 1: SYN synchronisation accuracy obtained for the whole considered test period

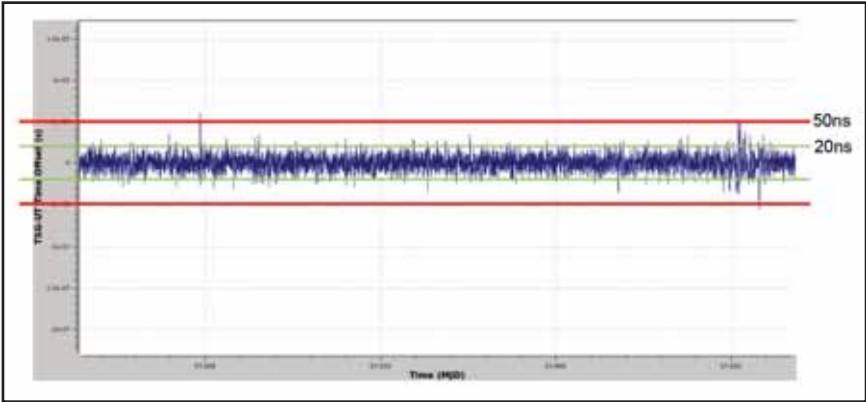


Figure 4: Phase offset between SYN and UTC(IT), over full test campaign period

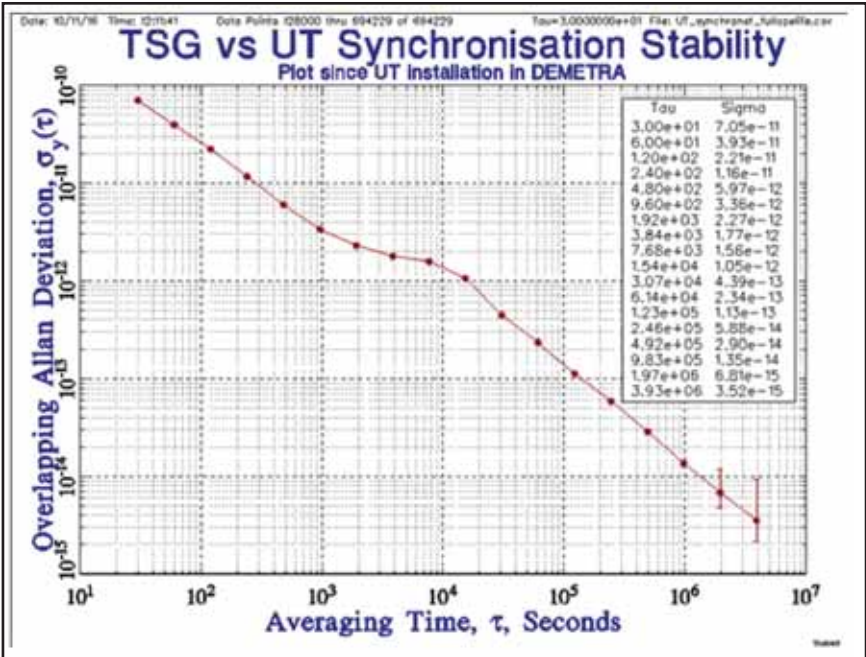


Figure 5: SYN overall synchronisation stability for the overall test period

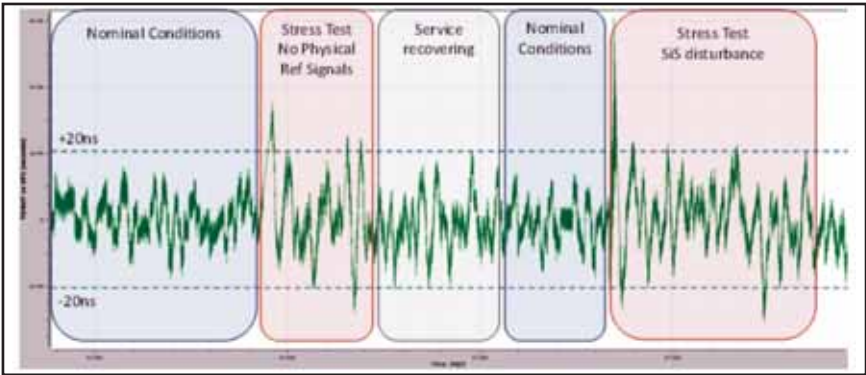


Figure 6: SynchroNet stress test period detail during DEMETRA campaign

of nominal conditions; this test labeled as “SiS disturbances” is the one in which a 16dB attenuation has been introduced by DEMETRA performance monitoring team at SYN GNSS receiver antenna and that caused a rather appreciable effect over time but at the same time shown that no jumps or output signals interruption was introduced and causing the phase alignment to slightly exceed nominal SLA threshold only for a short period before effects were compensated and nominal expected behavior restored.

Conclusions

DEMETRA experimentation provided a valuable test-bed for SynchroNet synchronization capabilities and benefitted independent performance evaluation and monitoring. Also, besides, technical aspects, it provided a rich insight in market and user needs and also reinforced in the conviction of the validity of a Time service oriented approach and revealed a large domain of potential users beyond that of GNSS ground segments for which SynchroNet was originally conceived and employed as part of GALILEO Test Range project of ASI(Agenzia Spaziale Italiana) and Regione Lazio.

SynchroNet exploits both the georeferenced network of nodes and internal steering algorithms to detect potential spoofing and to mitigate the effects of spoofing and jamming in terms of nodes synchronization accuracy and synchronization stability.

Also DEMETRA experience was useful to establish new opportunities on business side (on user side the idea of Time Services appears to have been receipt with interest and enthusiasm) as well as to identify new research areas and academic transversal cooperation.

In particular SynchroNet will be the basis for a study on securing and optimizing Energy Distribution networks based on Phasor Measurement Units that will explore currently used timing source security flaws, threats and their potential consequences as well as the revenues impact of a time service that is more secure and offering several order of magnitude accuracy and stability with respect to current requirements.

References

- [1] P.Tavella and ALL DEMETRA consortium by Aizoon, ANTARES, Deimos, Elproma, INRIM, Metec, NPL, ORB, Politecnico of Torino, Thales Alenia Space , UFE, Vega UK, and VTT, “The European Project DEMETRA, Timing services based on European GNSS: First experimental results” –IEEE Metrology for Aerospace, 2016 Florence (Italy)
- [2] D.B. Sullivan, D.W. Allan, D.A. Howe, F.L. Walls, “Characterization of Clocks and Oscillators”, NIST Technical Note 1337, Mar. 1990
- [3] M. A. Lombardi, L. M. Nelson, A. N. Novick, V. S. Zhang, “Time and Frequency Measurements Using the Global Positioning System”, Cal. Lab. Int. J. Metrology, pp. 26-33, (July-September 2001).
- [4] Q.Morante,M.Eleuteri,E. Variale.V.Valle,G.Pesci,F. Martinino,F.Gottifredi, “Galileo Test Range: Performance Test Results”, ION '08, San Diego (CA). ▲

HI-TARGET



iBoat BM1

Intelligent USV with brilliant mobility



Professional sounding module guarantees sounding range 0.15~300m



Ducted propellers avoid being twined by aquatic plants



Auto-return while low battery or dropped signal



Manual or autopilot , switchover by one step

BERLIN 2017 INTERGEO

26 - 28 SEPTEMBER

HI-TARGET Hall 1.1, C1.061

www.hi-target.com.cn | info@hi-target.com.cn

In Coordinates

10 years before...



mycoordinates.org/vol-3-issue-08-August-07/

Geospatial futurology

Robin Mannings
works in the Research
Department of BT

The final challenge will be to make things simple for people who just want answers to problems and some fun with minimum hassle. Maps (which many people find difficult) are increasingly touching the lives of citizens but in some ways we need to make the GIS disappear so the clever software does all the work.

NSDI-then, now and whenever

Mukund Rao
Former President, GSDI

Will our future generation view and know India only as these outside “initiatives” will portray? If we do not act now, we will be leaving a legacy for our future generation – who will feed on “outside view and offering” and will seldom believe that India also had the capability to establish map and image portals as part of a national infrastructure. It does hurt my conscience, many times. In that sense, I think the last of the chance for India for positioning a good leadership NSDI is just facing us. Make it happen now... or else there will be a good Indian spatial database (images are already there; maps also will be there soon; solutions will also follow soon later) from outside soon.

Managing land information

Brig M V Bhat
Addl Dir Gen Mil Svy, India

The efficiency of Land Information Management System will be assessed by its capacity to meet the needs of the land managers and users in urban and rural areas.

The benefits of future GNSS

**Yu-Sheng Huang, Yun-Wen Huang,
Kai-Wei Chiang**

A technical benefit of the geomatics and surveying industry in Taiwan is given in this article. The USA is modernizing GPS, Russia is refreshing GLONASS, and Europe is moving ahead with its own Galileo system. Extra satellites will make possible improved performance for all applications, and especially where satellite signals can be obscured, such as in urban canyons, under tree canopies or in open-cut mines. The benefits of the expected extra satellites and their signals outlined above can be categorized in terms of availability, accuracy, continuity, reliability, efficiency, and ambiguity resolution issues. All the performance indices given in this article strongly indicate the benefits of future GNSS.

GNSS data for ionosphere characterization

The increasing number of GNSS receivers enables comprehensive studies of ionosphere. Different products derived from calculated ionization levels give insight in ionospheric conditions and dynamics



Josip Vuković
Researcher at Innovation
Centre Nikola Tesla,
Zagreb, Croatia



Tomislav Kos
professor at
Department of Wireless
Communications,
Faculty of Electrical
Engineering and
Computing, University
of Zagreb, Croatia

Global Navigation Satellite Systems' (GNSS) performance is affected by ionosphere. Sudden variations in ionization levels can increase the pseudorange errors and even cause loss of lock on some of the visible satellites, lowering the positioning accuracy and availability. Logically, GNSS can benefit of deeper understanding of ionospheric behavior and the processes behind it. On the other hand, GNSS and their wide spread receiver networks are nowadays the main source of data on ionosphere, alongside ionosondes, low Earth orbit (LEO) satellites and incoherent scatter radars. The increase in the number of GNSS multi-frequency receivers which provide publicly available data, usually in Receiver Independent Exchange Format (RINEX), deepens our knowledge of ionosphere, possibly enabling better correction of ionospheric errors in the future.

GNSS derived ionospheric data

The ionospheric conditions are affected by local time, geomagnetic coordinates, season, solar activity and geomagnetic activity. Together, these factors influence the structure and ionization levels in the ionosphere. Even though GNSS

receivers do not provide data on ion composition in the ionosphere nor on the height of ionospheric layers and the associated electron density, they provide invaluable data which can characterize the ionospheric conditions. Signal phase and Signal-to-Noise Ratio (SNR) can be used to identify ionospheric scintillation, i.e. small plasma bubbles with density different than the surrounding plasma, which usually appear in polar and equatorial regions and can cause loss of lock on satellite signals. In order to provide indices on amplitude and phase scintillation, a 50 Hz or 100 Hz raw data output from GNSS receiver is required, but such receivers represent only a minority of all the deployed receivers, as the standard RINEX data rate is 30 s. On the other hand, Total Electron Content (TEC), which is proportional with the ionospheric signal delay, can be derived from any dual frequency receiver. The ionospheric error is usually quantified with TEC units (TECU), which equal 10^{16} electrons/m². One TECU on GNSS L1 frequency (1575.42 MHz) contributes with 0.16 m pseudorange error.

TEC is calculated for every satellite-receiver pair. In order to geotag it, based on receiver and satellite locations, coordinates of a point on the path between the satellite and the receiver, situated on height of 350 km are calculated. The height of 350 km is the height where the electron density in the ionosphere is the highest. Vertical TEC (VTEC), derived from Slant TEC (STEC), is pinned to the calculated coordinates.

Most of the receivers support multiple GNSS constellations. A receiver situated in low and middle latitudes can

Research communities in the fields of GNSS and ionosphere benefit of each other. GNSS are a powerful tool for ionospheric research, continuously providing data from around the world, with ever increasing number of available receivers.

usually receive signals from about 15 GPS and GLONASS satellites visible above the horizon, and slightly less towards the poles because of the constellation inclination in respect with the equatorial plane. With emerging BDS and Galileo systems, the number of visible satellites is even higher. Therefore, each GNSS receiver produces TEC data on 15 or more locations with different azimuths, and with distance up to 900 km from its location. Increasing the number of receivers increases the covered area and the density of points with calculated TEC, enabling interpolation and geographic representation of the collected data. Europe is a good example of a region well covered by GNSS stations with publicly available RINEX data, as can be seen in Figure 1.

VTEC values depict the current state of the ionosphere over a region of interest. In order to avoid appearance of faulty data, it is recommended to calibrate the values and to not to use data of satellites with low elevation, as such data are severely affected by multipath and mapping function errors. An example of the most commonly used GNSS data derived ionospheric product, a VTEC map, is shown in Figure 2. It is based on data of several GNSS receivers situated in southern Brazil and gives information on the current state of the ionosphere.

To further highlight the locations where ionization levels over neighboring sectors change the most, the TEC gradients can be used. Usually east-west and north-south TEC gradients are presented. Figure 3 represents such visualization, revealing the highest east-west gradients in the northeastern part of the observed region. That information can be useful to the users of differential GNSS or Ground Based Augmentations System (GBAS), as on locations with high TEC gradients the ionization levels for a referent receiver and an end user can be very different.

Even though TEC and its gradients provide very useful information, they lack the information on variability with time. Therefore, using only a TEC image it is not possible to conclude if the ionization levels change or remain the same, are the observed conditions usual for the area or not and are the disturbed regions moving or are they static. To answer those questions, TEC maps from different time epochs are needed. For instance, as presented on Figure 4, it is possible to observe the difference between current TEC values and its 10-day average. That difference reveals the areas of disturbed ionosphere and can indicate that single frequency GNSS receivers that rely on global ionospheric models will probably experience accuracy degradation in such regions.

In order to focus more on current ionospheric dynamics, Rate of TEC (ROT) can be used. ROT represents the amount of change of TEC in one minute. While TEC revealed the areas with the highest and the lowest ionization levels, ROT reveals the areas with the biggest change of TEC levels. Figure 5 shows ROT over Europe, calculated on points marked in red and interpolated in between. In non-disturbed ionospheric



Figure 1: European GNSS stations with publicly available RINEX data (UNAVCO, Inc.)

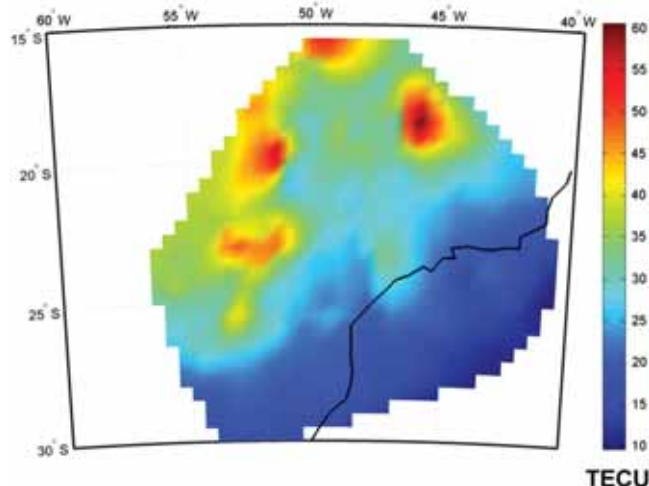


Figure 2: TEC over southern Brazil on February 12 2012, 03:10 UTC (Cesaroni et al., 2015)

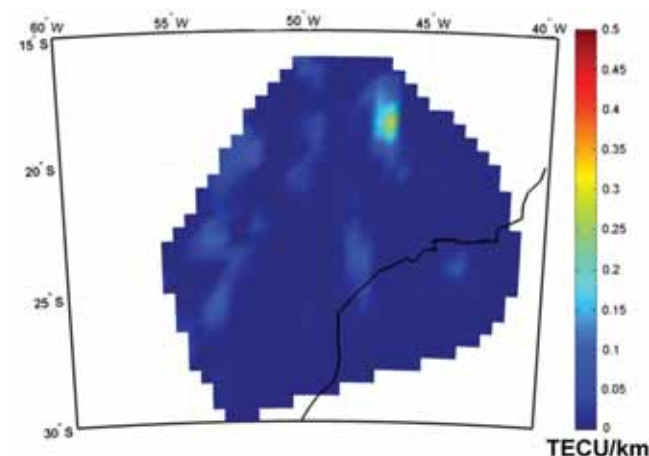


Figure 3: TEC east-west gradients over southern Brazil on February 12 2012, 03:10 UTC (Cesaroni et al., 2015)

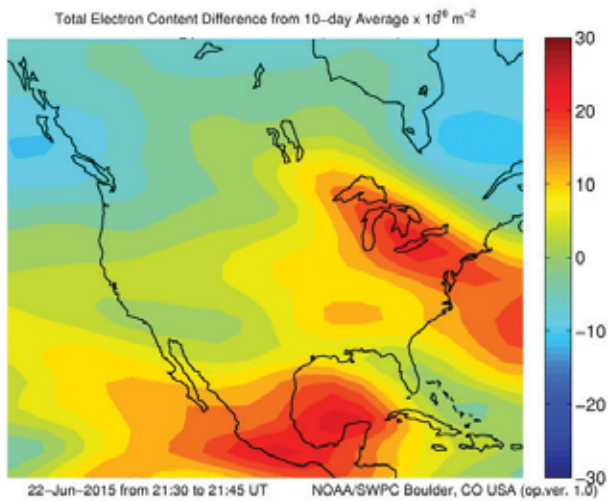


Figure 4: TEC difference from 10-day average over North America on June 22 2015, 21:30 UTC (NOAA/SWPC)

conditions the ROT values in middle latitudes are usually very low, but in depicted example a strong geomagnetic storm was underway, causing fast changes in ionization levels. The highest changes are observed in the northern part of the observed region, over Denmark, Scotland and Finland.

Spatial gradients of ROT can be calculated to show the trends in the ionospheric dynamics. The north-south gradients shown in Figure 6 are dominant in comparison with the east-west gradients shown in Figure 7, both reaching their maximal values in the area over Denmark. Over Scotland and Finland the ROT was high, but the levels increased gradually with distance and therefore the gradients remained low. In the areas with high ROT spatial gradients the neighboring regions experience different rate of change of ionization and the absolute values of TEC in these regions can also be expected to differ more in the following moments.

ROT Index (ROTI), a standard deviation of ROT during a 5-minute period can also be used to highlight areas with ionospheric irregularities, especially those smaller in size.

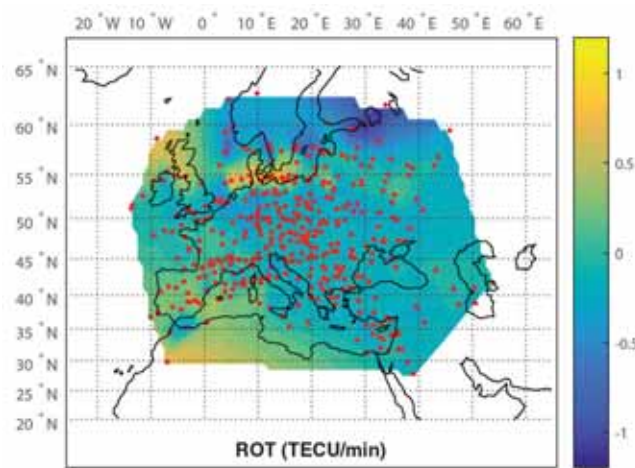


Figure 5: ROT over Europe on June 22 2015, 20:00 UTC (Vuković and Kos, 2016)

GNSS and ionosphere – Information cycle

Research communities in the fields of GNSS and ionosphere benefit of each other. GNSS are a powerful tool for ionospheric research, continuously providing data from around the world, with ever increasing number of available receivers. Public availability of the data and standardized data formats play key role in enabling ionospheric studies, comprehensive both in time-span and geographic coverage. The GNSS based ionospheric data can be further processed, creating TEC derived products which show the current state of the ionosphere, reveal its temporal dynamics and highlight the areas with the highest amplitudes of changes in ionization levels. Usually a combination of products

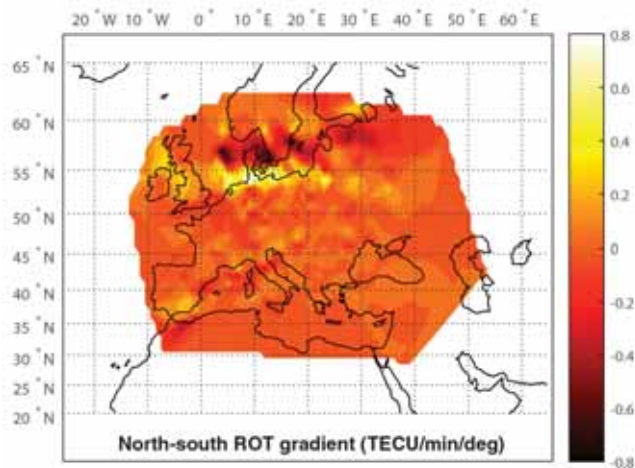


Figure 6: ROT north-south gradients over Europe on June 22 2015, 20:00 UTC (Vuković and Kos, 2016)

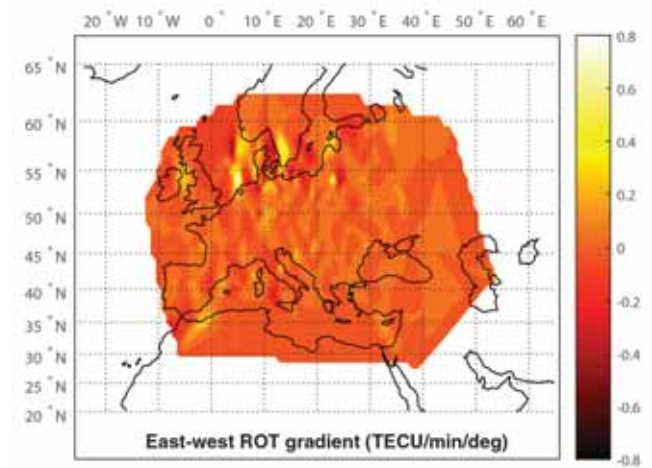


Figure 7: ROT east-west gradients over Europe on June 22 2015, 20:00 UTC (Vuković and Kos, 2016)

should be used as they complement each other. Based on such GNSS-data-based information the ionospheric models can be improved, the real-time data can be passed to the users and predictions on ionospheric conditions can be proposed. Finally, GNSS is the greatest beneficiary of better understanding the ionosphere, along with technology and business sectors relying on accurate GNSS based positioning, navigation and timing (PNT).

Acknowledgment

The research leading to these results has received funding from the European Community's Seventh Framework Programme (FP7/2007-2013) under grant agreement No. 607081.

References

- Cesaroni, C., Spogli, L., Alfonsi, L., De Franceschi, G., Ciruolo, L., Galera Monico, J. F., Scotto C., Romano, V., Aquino, M. and Bougard, B., (2015), "L-band scintillations and calibrated total electron content gradients over Brazil during the last solar maximum", *J. Space Weather Space Clim.*, 5, A36. doi: 10.1051/swsc/2015038
- NOAA/Space Weather Prediction Center, "Real-time US-Total Electron Content: Vertical and Slant - Difference from 10 day average indicating recent trend", Accessed on June 23 2015. http://legacy-www.swpc.noaa.gov/ustec/DIF_index.html.
- UNAVCO Inc., "Data Archive Interface v2". Accessed on June 6 2017. <http://www.unavco.org/data/gps-gnss/data-access-methods/dai2/app/dai2.html#>.
- Vuković, J. and Kos, T., (2016), "Ionospheric spatial and temporal gradients for disturbance characterization", *Proceedings of 2016 European Navigation Conference (ENC)*, Helsinki, pp. 1-4. doi: 10.1109/EURONAV.2016.7530564. ▴

Galileo update

ESA communication team hands off responsibility to GSA

After four years of work, the European Space Agency (ESA) team tasked with keeping the world informed on the status of the Galileo satellite navigation system has formally passed on its responsibility to a European Union agency. This shift is part of a wider transfer of responsibilities, as this month see the official handover of the running of the Galileo system from ESA to the European Global Navigation Satellite System Agency (GSA).

The very first Notice Advisory to Galileo Users (NAGU) was issued in June 2013, just three months after the first Galileo positioning fix was achieved, to a then small community of researchers and industrial users, interested in making tests with the newborn four-satellite constellation. A total of 189 NAGUs were issued under ESA oversight in the last four years, as the constellation grew to its current 18 satellites. The user base increased dramatically from 86 to 774 registered users on the European GNSS Service Centre website as companies worked to prepare Galileo-ready products and then, on 15 December 2016, Galileo's Initial Services began operating.

Europe's Galileo satnav identifies problems behind failing clocks

For months, the European Space Agency—which runs the programme—has been investigating the reasons behind failing clocks onboard some of the 18 navigation satellites it has launched for Galileo.

Each Galileo satellite has four ultra-accurate atomic timekeepers, two that use rubidium and two hydrogen maser. But a satellite needs just one working clock for the satnav to work—the rest are spares. Three rubidium and six hydrogen maser clocks were not working, with one satellite sporting two failed timekeepers.

"The main causes of the malfunctions have been identified and measures have been put in place to reduce the possibility of further malfunctions of the satellites already in space," commission spokeswoman Lucia Caudet said.

ESA found after an investigation that its rubidium clocks had a faulty component that could cause a short circuit, according to European sources.

The investigation also found that operations involving hydrogen maser clocks need to be controlled and closely monitored, the same sources said.

The agency has taken measures to correct both sets of problems, the sources added, with the agency set to replace the faulty component in rubidium clocks on satellites not yet in orbit and improve hydrogen maser clocks as well.

"The supply of the first Galileo services has not and will not be affected by the malfunctioning of the atomic clocks or by other corrective measures," Caudet said, and that the malfunctions have not affected service performance. Read more at: <https://phys.org>. ▴



• TRIUMPH-LS vs. R10*



- TRIUMPH-LS in use
- Ugly competition

see inside »



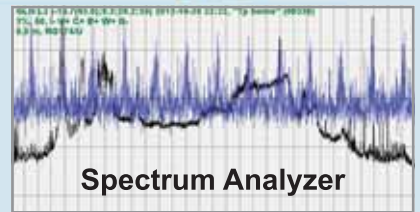
*R10 is trademark of Trimble



Monitor
document and
record the health
of your shots



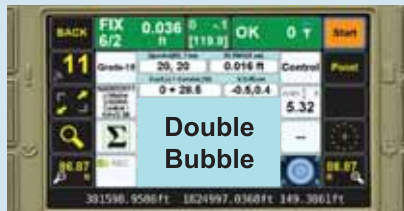
BEAST MODE RTK



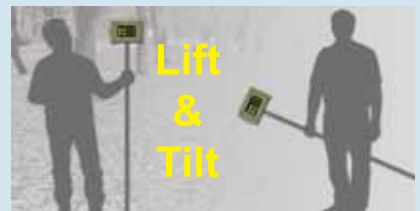
Spectrum Analyzer



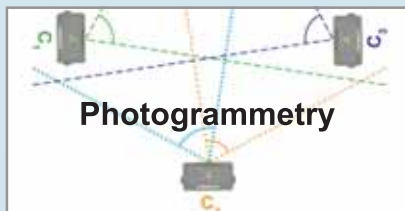
180-pound
Gorilla
Test



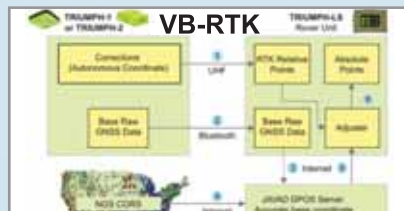
Double
Bubble



Lift
&
Tilt



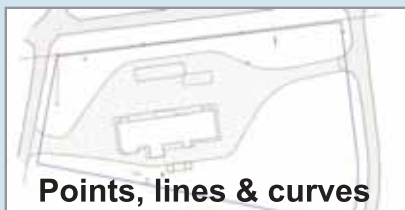
Photogrammetry



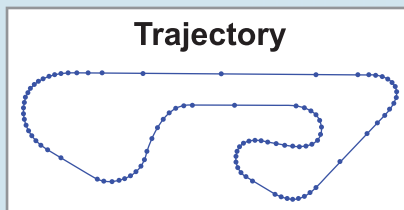
VB-RTK



Localizations



Points, lines & curves



Trajectory



Photo & audio

**REVERSE
SHIFT<<it**



TRIUMPH Chip

RAMS
Remote Assistance & Monitoring Services

For all others see www.javad.com

What Do You Use the TRIUMPH-LS For?

In some ways, I would use the LS for any of the items you list, but my specific work is boundary and topographic. About the only thing I won't use the LS for is precise vertical (hard surface topo for example) that requires better than a centimeter, particularly if I have to collect a lot of points with that accuracy requirement. This is pretty uncommon for my needs though.

I would use it for many types of construction layout. I don't do a lot of construction layout work though. It's the way to layout utility corridors.

Shawn Billings, PLS
Kilgore



The more fitting question for me would be what don't you use the LS for.

I even used it to set the locations for the post holes on my construction project and then drilled them. I did not have to shave out any of the holes. The posts went in perfectly.

The LS is a workhorse when it comes to open sky topo. I finished the field in just a few hours and never cut anything. I was able to crawl around and get to where I needed then let the LS work.

Adam Plumley, PLS

TRIUMPH-LS vs. R-10

Stephen K. Drake, PLS, CFedS

JAVAD TRIUMPH-LS rover, TRIUMPH-2 base, with spread spectrum radio, and a set of pods I have hiked up mountains all over the country, even at a 115 degrees in the desert, thankful the whole set weighs less than my R8 tripod.



Trimble R-10 rover, TSC3 controller, and R-8 base, with its bonus (heavy) tripod. (yea I want to hike that up the mountain for my setup...) The market heavy weights! (yea pun intended)

We used to be Azure Land Surveying in Kingman, Arizona. We have relocated to the North Coast of California where the **Redwood forests** thrive operating now as Lost Coast Land Surveying out of Eureka, California.

Desert surveying has it's unique challenges but really are light weights when compared to trying to obtain precise measurement in the coastal **rain forests**.

We are **veterans of Land Surveying** having experience in many jurisdictions, environments/eco-systems from the tropics in south Florida, upper Midwest forests, desert southwest, and Alaska's arctic and coastal rain forest environments. **40 years of wondering in the wilderness** to be sure. We have used **most of the equipment and methods from the top vendors**, including traditional methods which remain the normal methods used in this part of California for obvious reasons. 300' tall trees and dense underbrush in coastal mountains make using anything else almost useless. One could almost remain competitive with a Gurley mountain transit and chain.

We have discovered though that where GPS is even remotely possible, **the TRIUMPH-LS is far superior** to any other system in it's ability to remain useful in this challenging environment.

Time after time finding it able to produce even when a competitor's top unit failed. **I'd like to share an experience I recently had.**

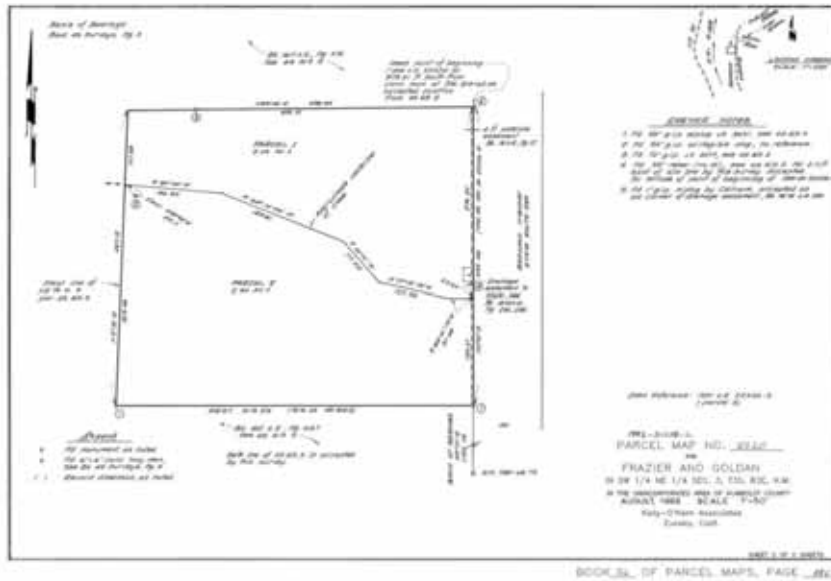
Back ground: ALTA survey in Miranda, California. After living on the north coast for a year and half, I returned to northern Arizona for a 1 year tour, I then returned to the north coast to support a new local survey effort with a company whose experience was elsewhere. Expectations where a little off to say the least. I was task to complete the job using the companies standard Trimble equipment set-up which in their opinion was second to none.

The site of this survey was 85% heavily wooded, mostly redwoods, steep terrain, and included a riparian boundary element, needing verification. Within an hour of being onsite I had the first monument recovered at the southeast corner of the parcel. **I tried in vain to get a position with the Trimble R-10 in my arsenal.**

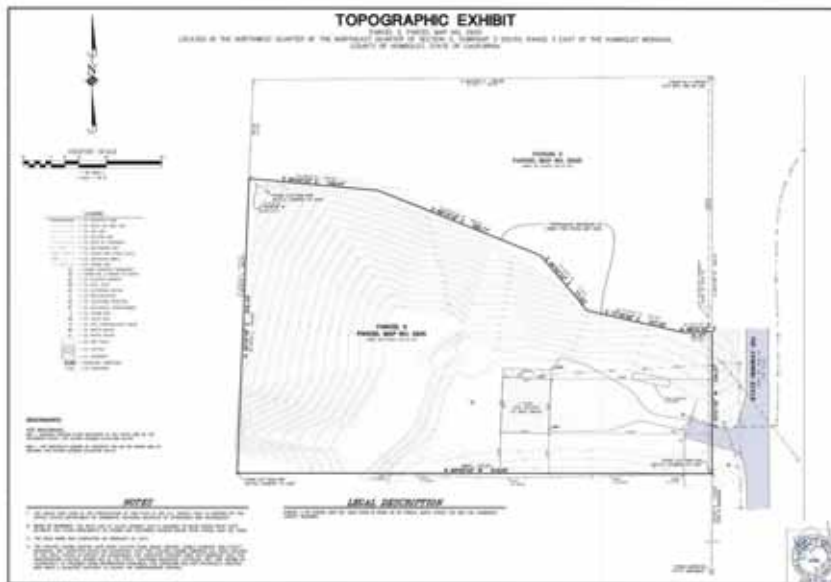
Well being the boy scout I was I was prepared for this. Having been a part of the JAVAD TRIUMPH beta program, discovering previously the benefit of this amazing machine in the forests, and desert mountains, already purchasing it, I carried it with me, just in case.

So I pulled it out knowing pretty much I would have a position somehow with it, but what's more, I decided it was a stellar opportunity for me to do **a side by side test.**

The survey:



The record parcel map from 1992 being retraced. Followed by the topo sheet from mine.



We did a survey sheet but the topo sheet shows terrain plus most of the survey data, the company name is removed to protect the innocent, if any, since this was not recorded.

You will see the southeast corner of the parcel, this being the first monument found, the controlling lines being the south line of the parcel and the tie to the 6x6 concrete right-of way monument to the south. We ended up within tolerance at 0.09' and 0.11' M vs. R.

R-10
occupying
southeast
corner.



No fix!
1m18
waiting
180
remaining
preset.



TRIUMPH-LS

same point.



Fix!

So with the TRIUMPH-LS I located the southeast corner of the parcel and verified it's record ties to the southwest corner and 6x6 monument to the south. The R-10 could not locate any.

Shot at the southwest corner. We got it with hybrid RTK PPK! Thank you Javad!



Shot at the 6x6 R/W monument. We got it RTK!





This is about 50' up creek from the northwest corner of the parcel. The reference point is about the center of this photo. We got it! Hybrid RTK. The creek is seen at the lower left of the photo, which is our north line, and the terrain and trees the same all the way to road, or worse.

Guess what? I located the creek and verified it to the record! Very rugged and tight canyon, but we got it!

And on a recent job, we got it!:



**Down in a
60 foot deep
canyon,
we got it!**

JAVAD GNSS Note:

Beware that R10 system is much much more expensive than the TRIUMPH-LS system. TRIUMPH-LS not only saves your job, your money too.

What a beautiful picture!

Have fun guys.



**Make lots of money
Twice as much!**

And how ugly competition can get!



A competitor's dealer at a state show takes one of our happy TRIUMPH-LS customers to his booth and tells him when Javad dies we will buy his company and close it.

How ugly a person can get! Instead of promoting innovation, he wants to kill it for his personal stupid benefits.

Also the idiot does not know of two things:

1. That I am healthy like a horse and have no intention to die anytime soon.
2. That JAVAD GNSS is not a start up company. Over 130 people working on the TRIUMPH-LS alone. It is a solid deep rooted institution which does not depend on any one person, including myself.

TRIUMPH-1M



864 channel chip, equipped with the internal 4G/LTE/3G card, easy accessible microSD and microSIM cards, includes "Lift & Tilt" technology.

TRIUMPH-2



Total 216 channels: all-in-view (GPS L1/L2, GLONASS L1/L2, SBAS L1) integrated receiver.

The one and the only Digital Radio Transceiver in the world!

Unique adaptive digital signal processing, which has benefits: the full UHF frequency range and all channel bandwidths worldwide • the best sensitivity, dynamic range, and the highest radio link data throughput • embedded interference scanner and analyzer • compatibility with another protocols. Cable free Bluetooth connectivity with GNSS receivers and Internet RTN/VRS access via embedded LAN, Wi-Fi, and 3.5G

And all this with competitive prices!

HPT435BT/HPT135BT/HPT225BT*



35 W UHF/VHF Transceiver

HPT404BT/HPT104BT/HPT204BT*



4 W UHF/VHF Transceiver

HPT401BT/HPT101BT/HPT201BT*



1 W UHF/VHF with internal battery

L-Band/Beacon*



Receivers for multiple applications

JLink 3G LTE BAT*



Web-interface Wi-Fi, Ethernet, 3.5 G, UHF/VHF/FH915, internal battery

OEM Solutions



902-928, 360-470, 225-255, 138-174 MHz

*Power, data cables and antenna are included.

PGM2016: A new Geoid Model for the Philippines

In 2016, the PGM2014 was re-computed into PGM2016 using the reprocessed and densified land gravity data (from 1261 to 2214 points)



R Gatchalian

Geodesy Division,
National Mapping and
Resource Information
Authority, Philippines



R Forsberg

National Space Institute,
Technical University of
Denmark, Denmark



A Olesen

National Space Institute,
Technical University of
Denmark, Denmark

In 2014, a preliminary geoid model has been computed for the Philippines i.e., Philippine Geoid Model 2014 (PGM2014), with the technical assistance of the National Space Institute, Technical University of Denmark (DTU-Space) using data from land gravity, airborne gravity, marine satellite altimetry and the newest satellite gravity data from the GOCE mission release 5. Digital terrain models used in the computation process was based on 15" SRTM data. The model is computed in a global vertical reference system then fitted to the ITRF GNSS/Leveling and validated with RMS value of 0.50m. In 2016, the PGM2014 was re-computed into PGM2016 using the reprocessed and densified land gravity data (from 1261 to 2214 points). Significant improvements can be seen in the reprocessed gravity data and GPS/Leveling (RMS = 0.040m). Further densification of the land gravity (in towns and cities) to 41,000 points will be conducted from 2017 until 2020 to refine the geoid. Re-computation will be done for the new version of the geoid as new gravity data comes in. *GRAVSOFT* system of FORTRAN routines developed by DTU-Space and Niels Bohr Institute, University of Copenhagen was used in computing the Philippine geoid.

called Vertical Datum. The universal choice of a vertical datum is the geoid – the reference surface for orthometric and dynamic heights (Vanicek, 1991). It is an equipotential level surface of the oceans at equilibrium, proposed by C.F. Gauss as the “Mathematical figure of the earth” (Dr. Bernhard Hofmann-Wellenhof, 2005).

With the advent of Global Navigation Satellite Systems (GNSS), it has become much easier to estimate Mean Sea Level (MSL) elevations using a geoid model. Applying a geoid model in GNSS surveys will eliminate the conduct of levelling. A geoid model is a surface (N) which describes the theoretical height of the ocean and the zero-level surface on land. In a



Figure 1: Philippine Vertical Control Network established by Levelling

Introduction

Vertical coordinates (i.e. Heights) of points are referred to a coordinate surface

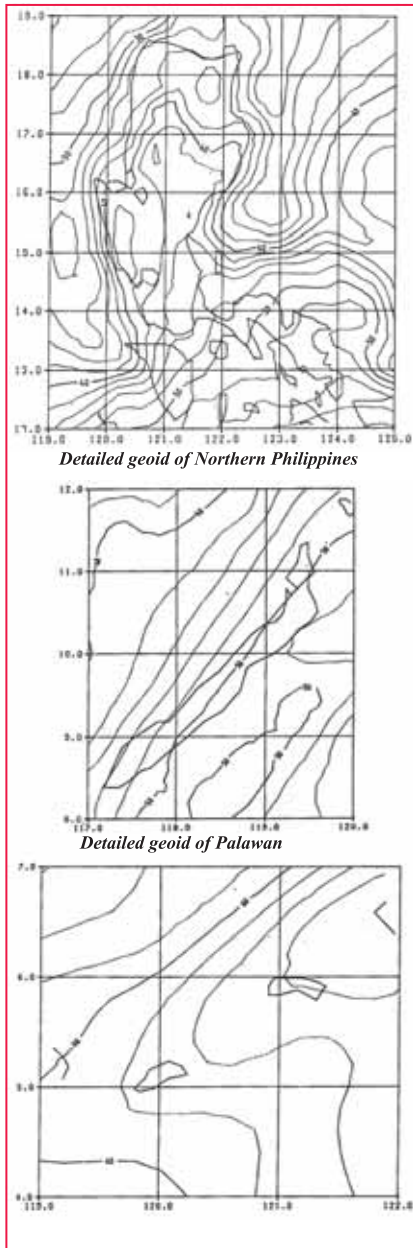


Figure 2: Detailed geoids of Northern (above) and Palawan with South West Philippines (below)

modern vertical reference system, the geoid is required to obtain orthometric height H ("height above sea level") from GPS by

$$H = h^{GPS} - N \quad (1)$$

Where h^{GPS} is the GPS ellipsoidal height, and H the levelled (orthometric) height.

In the Philippines, determination of elevation H of points and Benchmarks (BMs) was normally conducted thru Geodetic Levelling, a tedious process that hinders the densification of BMs during the early times.

In 2007, during the Philippine Reference System 1992 (PRS92) Campaign, 22,851 BMs were established along major roads nationwide with a maximum divergence of $4.0\text{mm}\sqrt{K}$ between two level runs (1st Order Accuracy). These first order level networks were connected to their respective reference tidal BMs to provide local MSL elevation. Figure 1 shows the Network of Level Lines with their corresponding Tide Gauge Stations.

The first attempt of computing a preliminary gravimetric geoid for the Philippines is through the Natural Resources Management Development Project (NRMDP) in 1991. Land gravity data and altimetrically-derived anomalies at sea and OSU89A to degree and order 360 (reference global model) were used. Biases between the gravimetric N and GPS/Levelling were found ranging from 2-6 m nationwide (Kearsley, 1991). Figures 2 and 3 shows the computed detailed geoids of the Philippines.

The making of Philippine Geoid Model 2016 (PGM2016)

In October 28, 2014 with the technical assistance of National Space Institute -Denmark Technical University (DTU-Space) and funding from National Geospatial-Intelligence Agency (NGA), a preliminary geoid model, Philippine Geoid Model 2014 (PGM2014) has been computed for the country using the data from land gravity, airborne gravity, marine satellite altimetry and the newest satellite gravity data from the GOCE mission release 5 with an accuracy of 0.30meters. In this paper, the computation of the PGM2014 will be discussed then its re-computation into PGM2016.

The airborne gravity survey

The success of the first long-range airborne gravity survey in Greenland 1991-92 by the group of US Naval research Laboratory, in cooperation with NOAA,

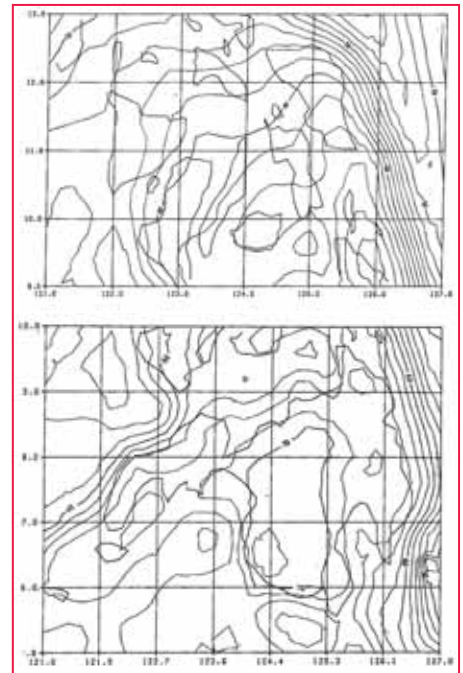


Figure 3: Detailed geoid of Visayas and Mindanao

NIMA and Danish National Survey paved the way for the use of airborne gravity in filling the intermediate wavelength bands between satellite gravity, e.g. GRACE and GOCE (R. Forsberg & Olesen, 2010) for accurate geoid modelling. There is now full operational capability of collecting seamless airborne gravity data across land and marine areas at 1-2 mGal r.m.s. accuracy and at around 4-6 km resolution due to the new gravity acceleration sensors and improved GPS processing methods.

After their successful airborne gravity campaigns in the other regions of the world (e.g., Malaysia, Mongolia, Ethiopia, South Korea, Nepal), DTU-Space conducted the airborne gravity survey in the Philippines on March until May of 2014 using a Cessna Caravan aircraft. This is part of the project to improve the global gravity field model EGM2008 under the umbrella of the NGA - Danish Geodata Agency BECA agreement. Figures 4 and 5 shows the aircraft used in the Philippine airborne gravity survey and its cabin layout respectively.

The following instruments were used:

- LaCoste and Romberg Air/Sea gravimeter S-38
- Chekan AM gravimeter #24
- Javad Lexion GPS receiver



Figure 4: The Cessna Grand Caravan aircraft used in the airborne survey



Figure 5: Cabin layout in the Cessna Caravan aircraft. To the right, the LCR gravimeter and behind it the Chekan meter

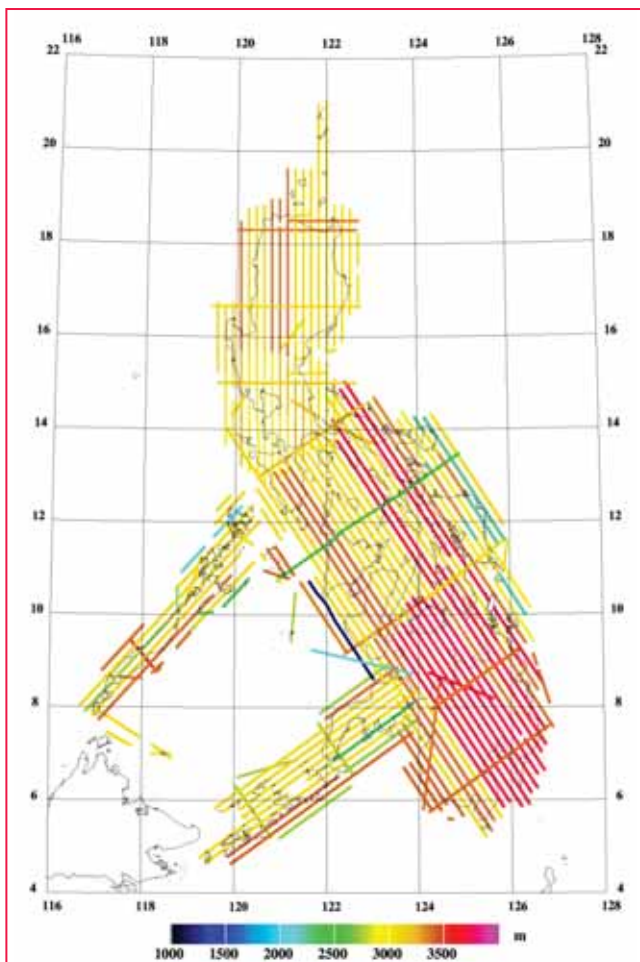


Figure 6: Flight track elevations of the airborne gravity survey

- Javad Delta GPS receivers
- Novatel dual frequency aircraft GPS antenna
- Power rack with DC/AC inverters, UPS etc.

GPS reference stations operated in all airports together with active geodetic stations of NAMRIA were used as base stations in computing the position of the aircraft. AUSPOS online positioning provides the coordinates of the reference stations (in ITRF2008) with an estimated accuracy of 0.50 to 2cm in vertical. Aircraft trajectories were computed with waypoint software package from Novatel (Calgary, Canada) using precise ephemeris from International GNSS Service (<http://igsb.jpl.nasa.gov/>). Parking spots were tied to NAMRIA first order gravity stations using Scintrex CG-5 gravimeter.

Mean altitude for all flights was 3185m with a terrain clearance of 545m above mountains and 3760m in lowlands. Figure 6 shows the color-

coded flight track elevations.

Free –air gravity anomalies at aircraft level are obtained from:

$$\Delta g = f_z - f_{z0} - h'' + \delta g_{eotvos} + \delta g_{tilt} + g_0 - \gamma_0 - \left(\frac{\partial \gamma}{\partial h} (h - N) + \frac{\partial^2 \gamma}{\partial h^2} (h - N)^2 \right) \quad (2)$$

Where f_z is the gravimeter observation, f_{z0} the apron base reading, h'' the GPS vertical acceleration, δg_{eotvos} the Eotvos correction computed by the formulas of Harlan (Harlan, 1968), g_0 the apron gravity value, γ_0 normal gravity, h the GPS ellipsoidal height and N the geoid undulation from EGM08 2.5x2.5minutes, γ_0 and the second order height correction is based on GRS80 definitions (Moritz, 1980). All altitude dependent atmospheric correction has been applied, see e.g. Hintze, et al. 2005. The platform off-level correction δg_{tilt} is based on a platform modelling approach described in (Olesen, 2002). All data were filtered with a symmetric second order Butterworth filter with a half power point at 170 seconds, corresponding to a resolution of 6km (half-wavelength).

Apron base readings were performed each day after the flight and approximately every second day before the flight to monitor drift of the gravimeter and for proper connection of airborne readings to the gravity network.

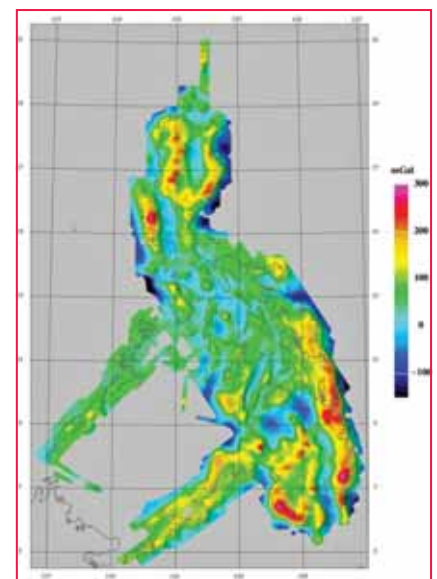


Figure 7: Free air anomalies gridded and with artificial shade highlighting short wavelength features

Table 1: Data statistics and residuals

Unit: mGal	Mean	Std. Dev.	Minimum	Maximum
Airborne	66.3	65.7	-168	293
GOCE R5-Direct residuals	3.2	41.6	-126	191
EGM08 residuals	1.1	15.6	-56	135

Figures 7 and 8 shows the gridded and acquired free air anomalies at flight altitude. Colour agreement at cross lines indicate consistent data. Closer examination of the misfit in the 289 line intersections shows a 3.7 mGal RMS error indicating 2.6 mGal average noise level.

Comparison to EGM08 shows significant differences in many places amounting to more than 130mGal over SE Mindanao, see Table 1 and figures 9 and 10.

Gravimetric geoid computation – principles

The PGM2014 is computed by the *GRAVSOFT* system, a set of Fortran routines developed by DTU-Space and Niels Bohr Institute, University of Copenhagen (Forsberg R, 2008). It forms the base of major recent geoid computation projects, such as the joint Nordic “NKG” geoid models, undertaken as joint geoid model computations of the Nordic and Baltic countries (R. Forsberg, D. Solheim & J. Kaminskis, 1996) under the auspices of the Nordic Commission for Geodesy (NKG), as well as the OSGM02 geoid model

of the UK and Ireland (R. Forsberg et al., 2002), and several national geoid models done from airborne surveys in recent years (Malaysia, Mongolia, Indonesia and others).

The “remove-restore” technique was used in computing the geoid, where a spherical harmonic earth geopotential model (EGM/GOCE combination) is used as a base. The geoid is divided into three parts namely: the global contribution N_{egm} , a local gravity derived component N_2 , and a terrain part N_3 .

$$N_{grav} = N_{egm} + N_2 + N_3 \quad (3)$$

The Remove – Restore Steps as illustrated by PAHLEVI, PANGASTUTI, SOFIA, and KASENDA (2015) are:

Remove Steps: Gravity measurement data is subtracted with global gravity anomaly and surface correction

$$\Delta g_{res} = \Delta g_{FAA} - \Delta g_{egm/goce} - \Delta g_{terrain}$$

1. Extract gravity anomaly from the spherical harmonic model to produce $\Delta g_{egm/goce}$ (Long wavelength)
2. Extract gravity anomaly from SRTM data to produce $\Delta g_{terrain}$ (short– medium wavelength)

3. Subtract gravity anomalies

$\Delta g_{egm/goce}$ and $\Delta g_{terrain}$ from Δg_{FAA} (measured gravity) to get Δg_{res}

4. Apply FFT to Δg_{res} to obtain geoid residuals ΔN_{res}

Restore Steps: Geoid residuals

summed with global geoid undulation and indirect effect, resulting to geoid height (Undulation), $N_{geoid} =$

$$\Delta N_{res} + \Delta N_{egm/goce} + \Delta N_{terrain}$$

1. Compute global geoid undulation from egm/goce $\Delta N_{egm/goce}$
2. Compute the terrain part $\Delta N_{terrain}$ from SRTM data
3. Sum up ΔN_{res} (from remove steps), $\Delta N_{egm/goce}$, and $\Delta N_{terrain}$ to obtain N_{geoid}

The spherical harmonic expression as a function of latitude, longitude and height is of the form:

$$N(\phi, \lambda, r) = \frac{GM}{Ry} \sum_{n=2}^N \left(\frac{R}{r}\right)^n \sum_{m=0}^n (C_{nm} \cos m\lambda + S_{nm} \sin m\lambda) P_{nm}(\sin \phi) \quad (4)$$

where G, M are γ earth parameters. The EGM08/GOCE combination model used involves more than 4 million coefficients C_{nm} and S_{nm} derived from very large set of global satellite data and regional (average) gravity data from all available sources, both open-file and classified, for details see <http://earth-info.nga.mil/GandG/wgs84/gravitymod/egm2008/index.html>.

The EGM08 model is incorporating GRACE satellite data, which determines the error spectrum of the EGM08 up to spherical harmonic degree 80 or so. New

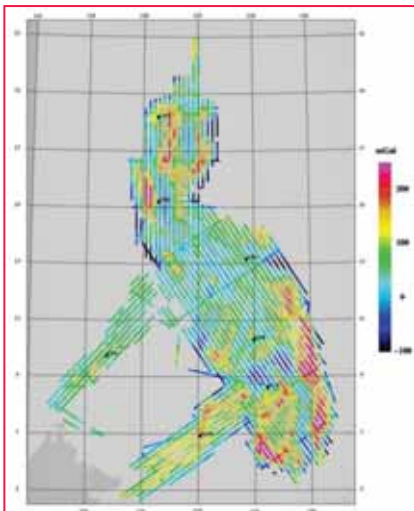


Figure 8: Free air anomalies at altitude

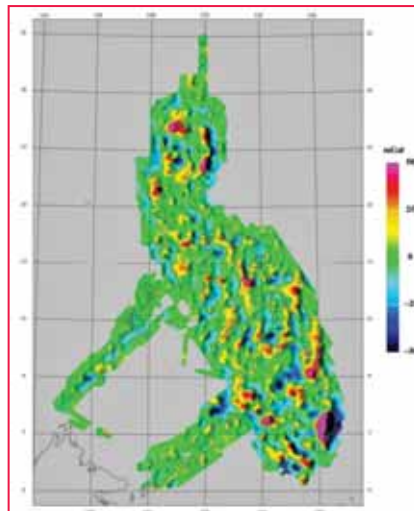


Figure 9: EGM08 residuals at altitude

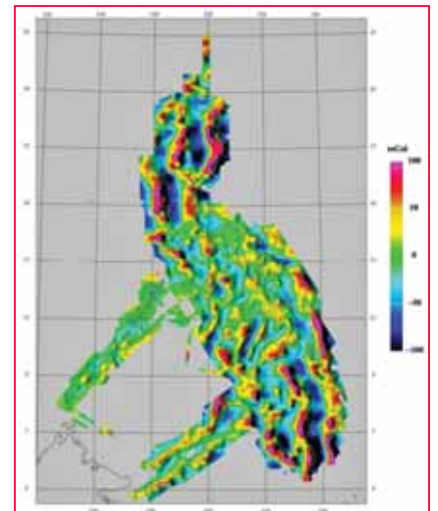


Figure 10: GOCE R5-Direct residuals at altitude

satellite data from the GOCE mission have recently been made available by the European Space Agency, for details see www.esa.int/goce. The latest GOCE spherical harmonic model (“Direct” Release 5 model), complete to degree and order 280 was used to update EGM08 field in the following way:

- EGM08 used unchanged in spherical harmonic orders 2-80, and from 200 up
- GOCE R5 direct model used in band 90-180
- A linear blending of the two models done in bands 80-90 and 180-200

The mixed spherical harmonic model (termed EGM08/GOCE) has been used to spherical harmonic degree $N = 720$, corresponding to a resolution of $15'$ or approximately 28 km. From the recent DTU geoid projects in France (Auvergne), Malaysia, and Nepal, this resolution appears to be a good “trade off” between the full resolution of EGM08 (degree 2160) and the local gravity data. Because the full-resolution gravity data used in the construction of EGM08 is classified, there is no good information on the quality of the errors in EGM08 at the high wavelengths in SE Asia, and only $15'$ mean gravity data are assumed to be underlying EGM08. All spherical harmonic computations were done in a grid using the *geocol17* program in grid mode.

The terrain part of the computations were based on the RTM method, where topography is referred to a mean elevation level, and only residuals relative to this level is taken into account. The mean elevation surface were derived from the SRTM $15''$ detailed model through a moving average filter with a resolution of approximately $20'$ (37 km; slightly longer than the $15'$ data resolution implied by spherical harmonic degree 720, in order to have a more smooth residual gravity signal Δg_2). The difference in resolution between reference field and RTM is *not* a theoretical issue, as the remove-restore method takes any “double accounted” topography into account fully.

The method for the gravimetric geoid determination is *spherical FFT* with

optimized kernels. This is a variant of the classical geoid integral (“Stokes integral”), in which there is a proper weighting of the long wavelengths from EGM08 and the shorter wavelengths from the local gravity data. Mathematically it involves evaluating convolution expressions of form

$$N_2 = S_{ref}(\Delta\varphi, \Delta\lambda) * (\Delta g_2(\varphi, \lambda) \sin\varphi) = F^{-1}(F(S_{ref})F(\Delta g_2 \sin\varphi)) \quad (5)$$

Here S_{ref} is a modified “Stokes” kernel, $\Delta g_2 = \Delta g - \Delta g_{egm}$ is the EGM08/GOCE-reduced free-air gravity anomalies, and F is the 2-dimensional Fourier transform operator. For details see references (R. Forsberg, D. Solheim & J. Kaminskis, 1996), (R. Forsberg et al., 2002) and (R. Forsberg & Olesen, 2010).

The geoid is computed on a grid of $0.025^\circ \times 0.025^\circ$ resolution (corresponding to roughly 2.7×2.5 km grid). The area of computation is 04° - 22° N and 112° - 128° E, covering the Kalayaan Islands of West Philippine Sea. Computations was based on least squares collocation and Fast Fourier Transformation methods which involve 1440×1280 grid points corresponding to 100% zero padding. The data are gridded and downward continued by least squares

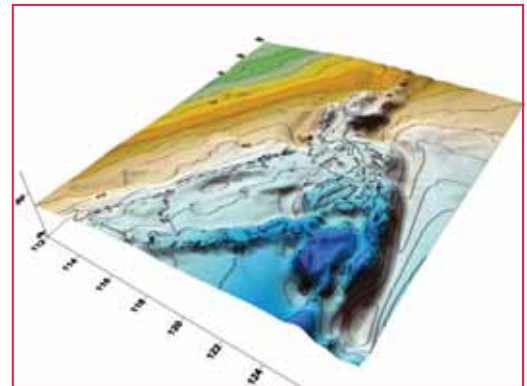


Figure 11: The Preliminary Philippine Geoid 2014 (PGM2014). Contour interval 5m

collocation using the planar logarithmic model. GRAVSOFT programs such as *gpcoll*, *spfour*, *gcomb*, *geoip* are involved in the process. Figure 11 shows the PGM 2014 at 5m contour.

The final gravimetric geoid solution was computed by the following steps:

- Subtraction of EGM08GOCE spatial reference field (in a 3-D “sandwich mode”)
- RTM terrain reduction of surface gravimetry, after editing for outliers
- RTM terrain reduction of airborne gravimetry
- Reduction of DTU-10 satellite altimetry in ocean areas away from airborne data
- Downward continuation to the terrain level and gridding of all data by least-squares collocation

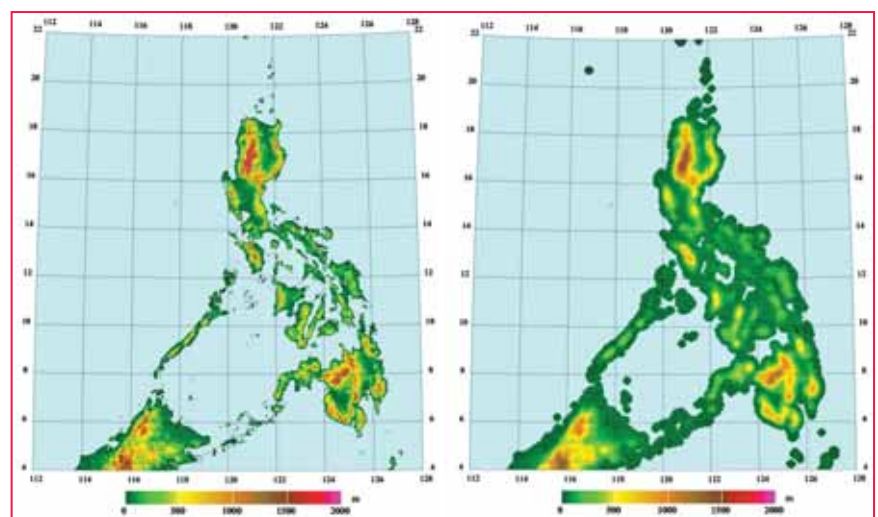


Figure 12: SRTM DEM data (left); low-pass filtered mean elevation surface (right), used as reference in RTM terrain reductions. Elevations in meters. Ocean depths are not used in the Philippines geoid computations.

using a $1^\circ \times 1^\circ$ moving-block scheme with 0.6° overlap borders

- Spherical Fourier Transformation from gravity to geoid
- Restore of RTM and EGM08GOCE effects on the geoid
- Correction for the difference between quasigeoid and geoid (using a Bouguer anomaly grid)
- Shifting of the computed geoid by +80 cm to approximately fit to Manila tide gauge datum

Data used and Quality Control for the geoid computation

The PGM 2014 is based on the following data:

- Airborne gravity data
- Land gravity from NAMRIA, reformatted to GRAVSOFT and mildly edited
- DTU10 global gravity anomalies from multi-mission satellite altimetry (Selected only in the open ocean area, away from the airborne gravity)
- SRTM 15" DEM data for the region
- EGM08 and GOCE RL5 satellite data

Some plots of the used and processed data are shown in the Figures 12-14.

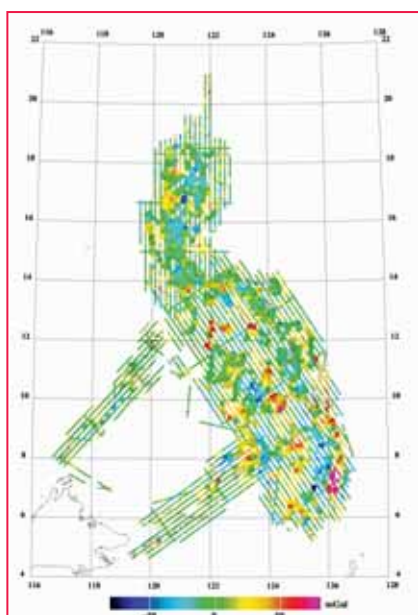


Figure 13: NAMRIA land gravity data and the airborne gravity data after terrain and EGM-reduction. Some outliers were deleted in the geoid processing.

Table 2: Statistics of remove steps in the PGM2014 computation (mGal)

Unit: mGal	Mean	Std.dev.
NAMRIA edited land gravity data (1261pts)	8.7	24.7
- above minus EGM08GOCE and RTM	0.9	21.4
Airborne gravity data (58515 pts)	1.5	20.7
- above minus EGM08GOCE and RTM	1.6	18.6
DTU10 altimetry gravity (28841 selected pts)	-9.6	12.3
- above minus EGM08GOCE and RTM	-0.3	10.8

Table 3: Statistics of the restore quantities on the geoid

Unit: meters	Mean	Std.dev.	Min.	Max.
Reduced geoid (after spherical FFT)	0.00	0.25	-1.61	2.88
RTM restore effects (computed by FFT)	0.00	0.04	-0.23	0.74
Final gravimetric geoid statistics	39.06	18.36	-9.02	76.43

The available data from the airborne and surface sources were quality controlled through plotting of the EGM08/GOCE and terrain reduction residuals, showing a few ($< 1\%$) obvious surface gravity outliers, which were deleted in the final geoid processing. The overall EGM/GOCE and RTM terrain “reduce” statistics for the data are shown in Table 2. Overall this statistics is good, with relatively small bias and standard deviation for all data sets.

restore geoid processing (“*geoid.gri*”), computed with full 3-dimensional modelling, going via the quasigeoid to the classical, final geoid.

The final geoid covers the region $4-22^\circ\text{N}$, $112-128^\circ\text{E}$, and has a resolution of $0.025^\circ \times 0.025^\circ$. The airborne and surface gravity data were gridded by spatial least squares collocation (*gpcoll*, using covariance parameters $\sqrt{C_0} = 18$ mgal, $D = 6$ km, $T = 30$ km). A priori errors assumed were 2 mGal for both the airborne data and the surface data (averaged in 0.025° blocks), and 5 mGal for DTU-10. The collocation downward continuation was done in $1^\circ \times 1^\circ$ blocks, with 0.6° overlaps.

Geoid processing results

The plots in the sequel shows the intermediate results of the final remove-

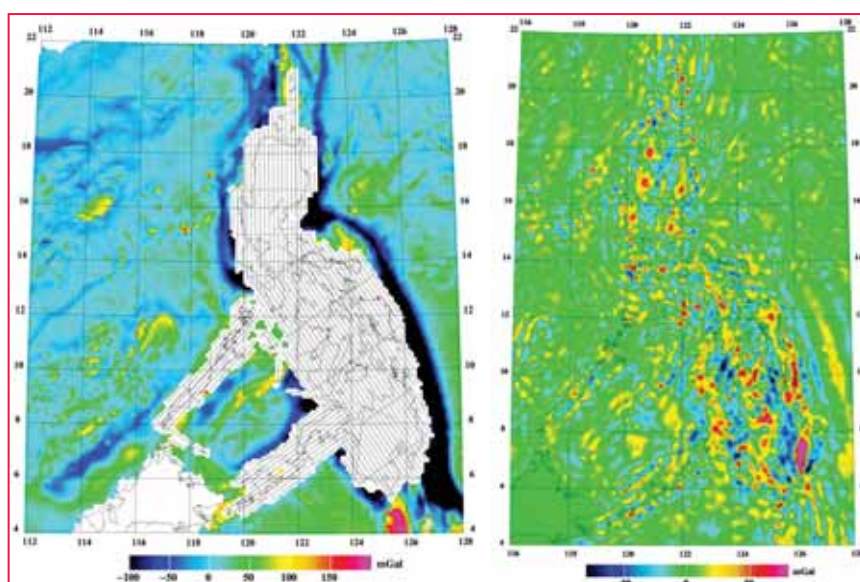


Figure 14: The used DTU-10 satellite gravity (left), and the collocation downward continued merged grid (right)

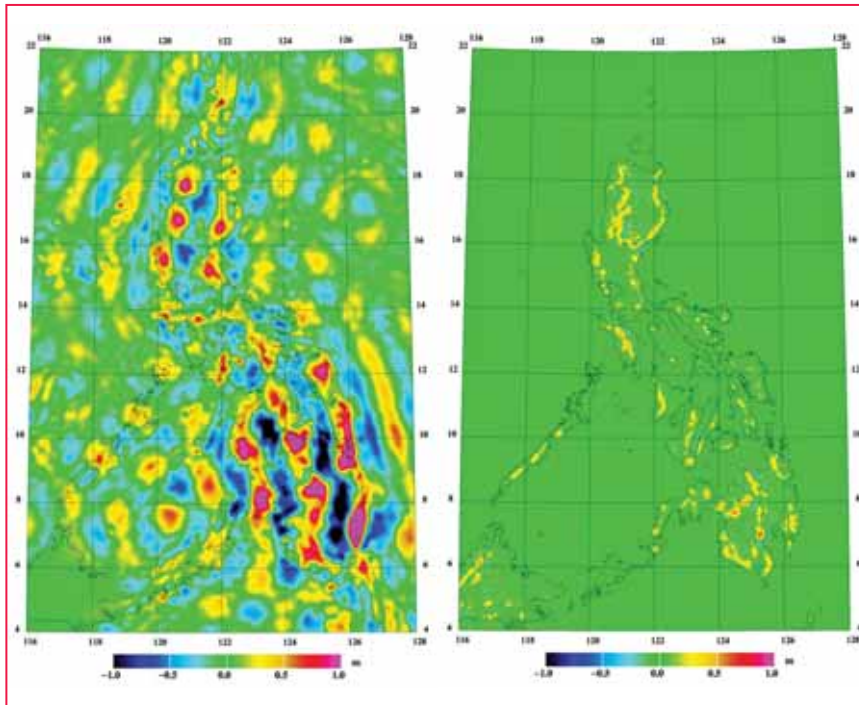


Figure 15: Left: Reduced geoid (after spherical FFT transformation); right: RTM terrain effect on the geoid

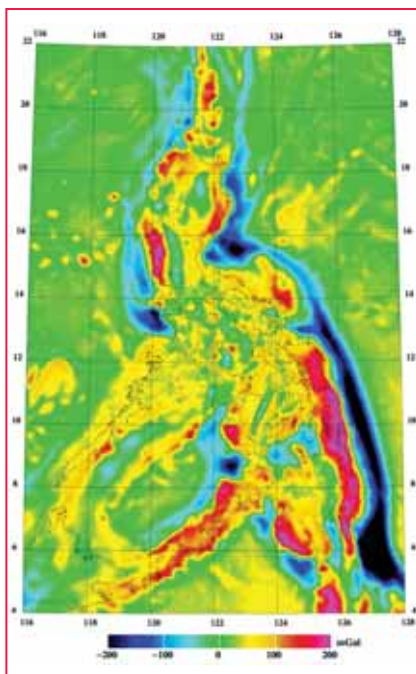


Figure 16: Bouguer anomaly grid, derived from the reduced data. Used for the geoid-quasigeoid estimation

For the spherical FFT transformation of gravity to geoid, 3 reference bands were used. Figure 15-16 shows the primary data grids done in connection with the geoid processing. The final geoid “restore” statistics is shown in Table 3.

GPS/Levelling data comparison and fitted geoid

A set of 190 GPS data in ITRF2005 levelling benchmarks was used to compare with the final geoid. These GPS data showed large errors relative to the geoid, with large outliers in some regions, likely due to a combination of geodynamic effects, levelling and GPS errors. The rms fit is 0.5 m; it is therefore not possible to use these data for validation of the geoid. Figure 17 shows the offset values, and the geoid correction surface for a fitted geoid *ph_geoid_fit* (corrector surface gridded with 80 km correlation length, and GPS-levelling apriori error of 10 cm). Fig. 18 shows the PGM2014 comparison to EGM2008; large improvements are seen, especially in the south. Fig. 19 shows a comparison to the DTU10-MSS, i.e. the MDT, shifted by -91 cm to take into account the different reference systems.

The PGM2014 files are given as *GRAVSOFT* grids, and can be interpolated by the GUI program *grid_int* (or the command line program “*geoid*”), provided to NAMRIA as part of the computations, along with the general software and geoid job setups (Appendix 1).

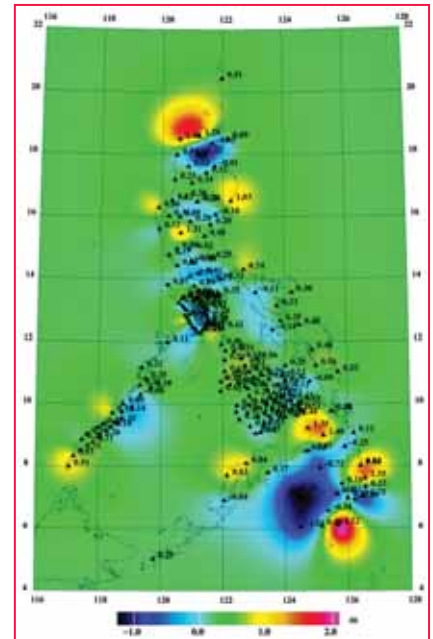


Figure 17: Location of GPS/Levelling data. Colour show the correction surface for the fitted geoid

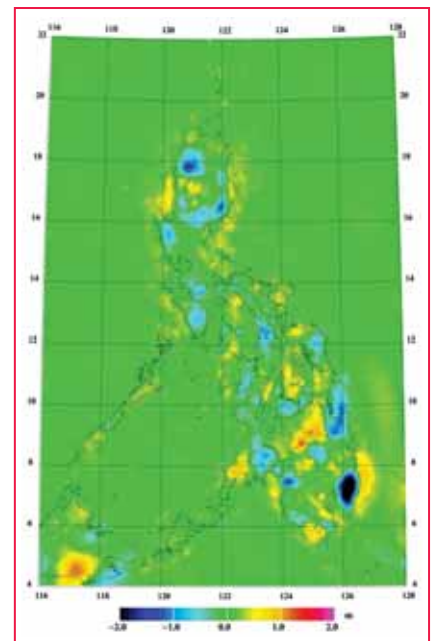


Figure 18: Differences between the PGM2014 and EGM2008

Re-computation of the geoid

To further improve a geoid model, Professor Forsberg in his paper “Towards a cm-geoid in Malaysia” (R. Forsberg, 2003) recommends the following:

- Levelling networks must be carefully analysed for adjustment errors

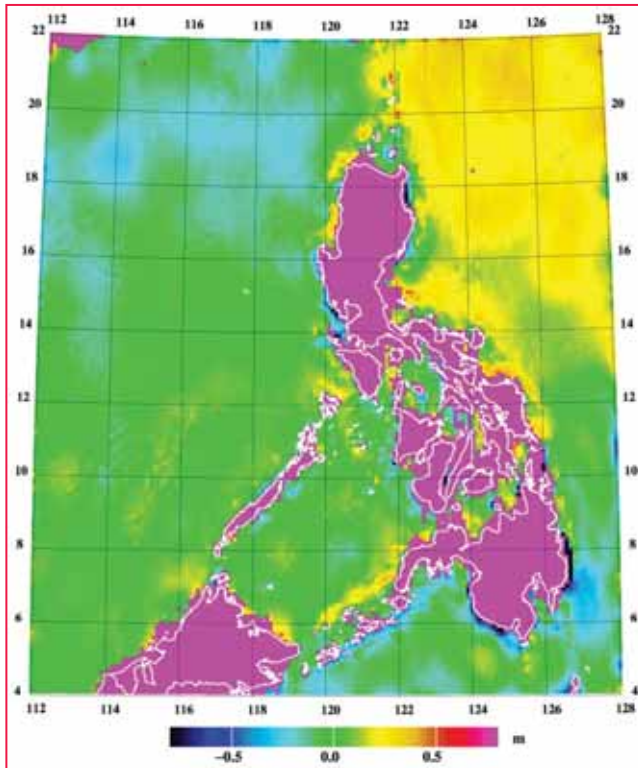


Figure 19: Mean Dynamic Ocean Topography (MDT) from DTU-10 mean sea surface (shifted by 91cm)

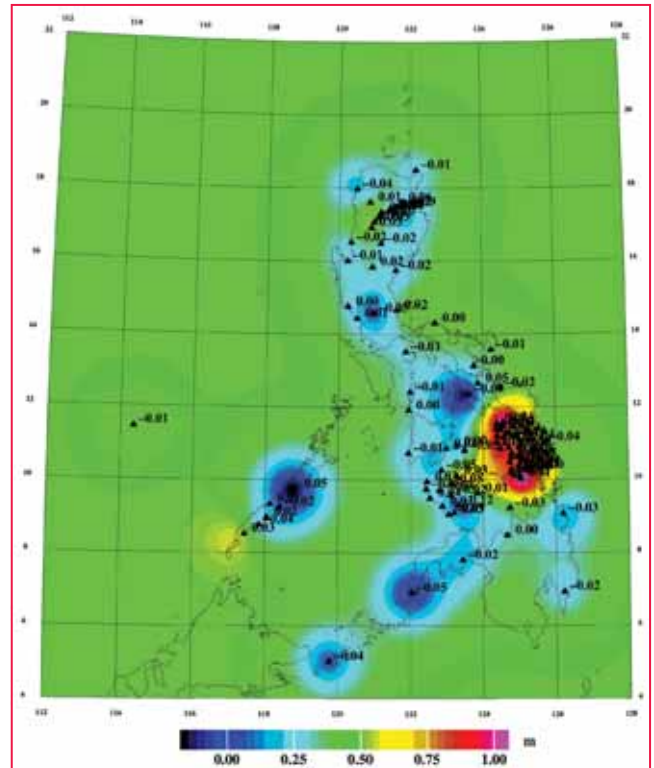


Figure 21: New correction surface of the fitted geoid (fitgeoid-itr2016)

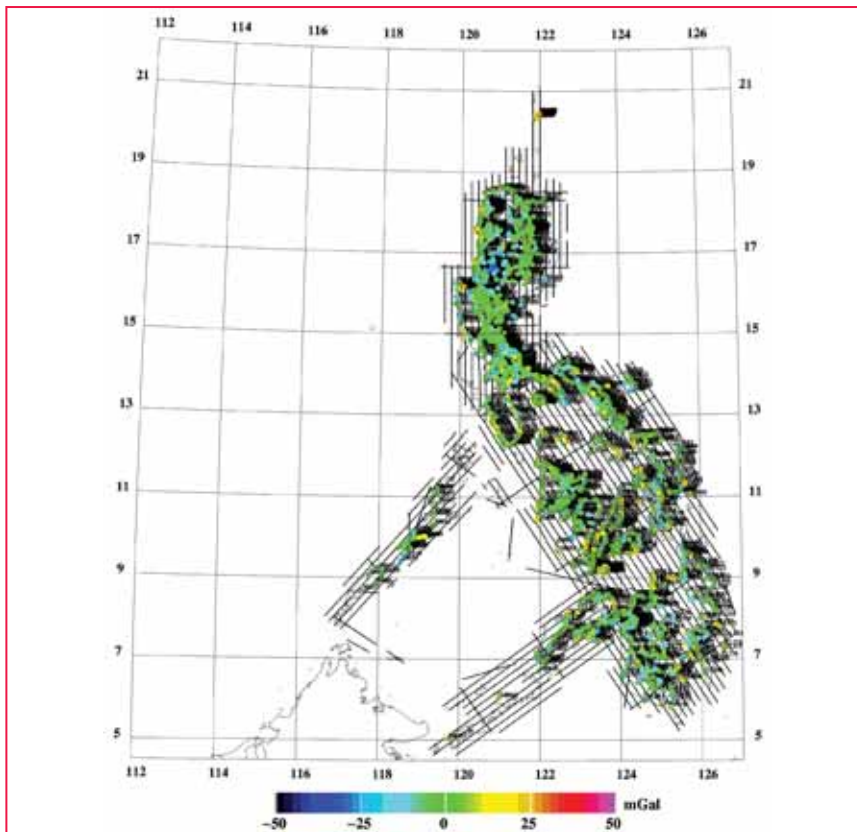


Figure 20: Land gravity data after reprocessing and densification (2214 points), plotted with the airborne data. Most differences are below 25mGals, although there are some points that exceeds 35mGals in mountainous regions.

- Connections and antenna height errors of GPS data on benchmarks must also be revisited and re-analysed
- Erroneous points (geoid outliers) must be resurveyed by Levelling and GPS
- New GPS-fitted version of the geoid must be computed as new batches of GPS-Levelling data, additional gravity surveys in major cities and GPS users height problem reports comes in.

In 2015 NAMRIA started the re-computation of the PGM2014 with the help of Professor Forsberg. The densification of land gravity stations was conducted in some major cities of the country. Also, the GPS-levelling data was re-analysed, corrected and outliers deleted.

Land Gravity Data

In this re-computation, the original airborne and satellite data processing results were used, only the densified land gravity data (2214 points to date) were reprocessed and quality controlled. Figure 20 shows the new plots of the land and airborne gravity data. Significant

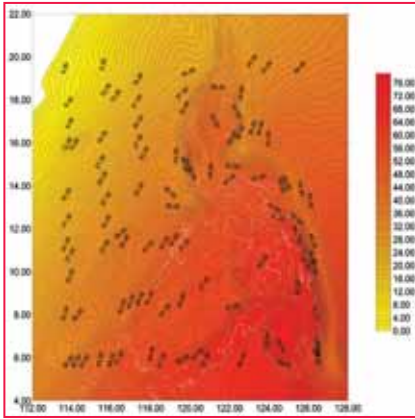


Figure 22: The new PGM2016.
Contour interval 1m.

improvements can be seen in the land data (thicker dots). Most dots are in green, some yellows and light blue (i.e., 25-50 mGals difference in mountainous areas).

GPS/Levelling Data

101 out of the 190 GPS/Levelling data on BMs remain (after cleaning up for outliers) and used as validation points.

After fitting the new GPS/Levelling, the RMS now is 0.054m with a minimum and maximum offset value of -0.124m and 0.169m respectively. This improvement is mainly due to the removal of erroneous levelling points. More points will be added to the GPS/Levelling data as the re-adjustment of the levelling network progresses. Figure 21 shows the offset values and the new geoid correction surface for the ITRF-fitted PGM2016.

Philippine Geoid Model 2016

The PGM2014 was re-computed to the new PGM2016 using additional land gravity stations combined with the same airborne and satellite gravity data. More land gravity data (up to 41,000) will be added from 2017 until 2020 in order to re-compute a new version and further refine the Philippine geoid. Figure 22 shows the new PGM2016 and its plotted differences with PGM2014 in figure 23. There are differences in most parts of the country as big as 0.30m.

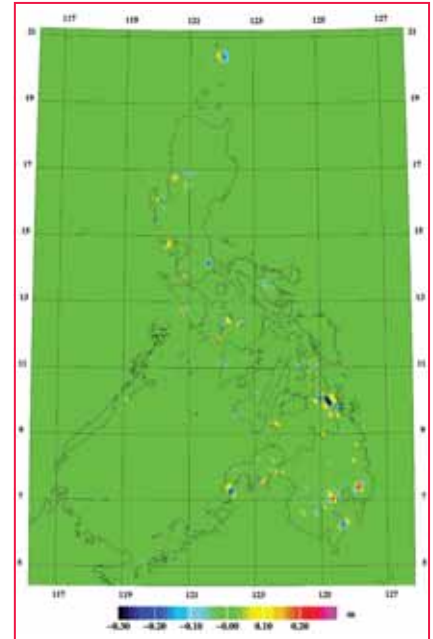


Figure 23: Differences between 2014 and the new 2016 geoid (ph_geoid files)

References

Dr. Bernhard Hofmann-Wellenhof, D. H. M. (2005). Physical Geodesy (pp. 46).

POWER AND PRECISION

EZSurv® GNSS post-processing software to compute high-quality positioning results at your fingertips!



MAPPING



SURVEY



UAV

Ask for your free trial > effigis.com/ezsuv

Appendix 1 – Directory structure and GRAVSOFT geoid jobs

Directory	Files	Comments
DATA	dtu-10_edited.fa	DTU-10 free-air anomaly data
	namria_edited.fa	NAMRIA edited free-air anomalies
	airborne.fa	Airborne free-air data
NAMRIA	namria.fa	Original NAMRIA gravity data, reformatted from xls- files
	gps-lev.dat	Files with N from GPS-levelling
	gps-lev-wgs84.dat	
DEM	ph_dem005.gri	SRTM 15" file (30" used in Malaysia)
	ph_dem025.gri	Averaged file for remote zone computations + geoid
	ph_demref.gri	RTM mean elevation surface, made with dem_ref.job
RD-TC	Remove steps (run "jobs" in sequence)	
	egm08goce5_720	Spherical harmonic coefficients for EGM08GOCE model
	geocol17.job	Program to compute EGM08GOCE in grids for N and g
	rd_surface.job	EGM and terrain reduction of NAMRIA data
	rd_air.job	Reduction of airborne data, incl. terrain effect filtering
	rd_dtu10.job	Reduction of DTU-10
	qc.job	Geogrid job to make difference NAMRIA minus airborne g
DOWNCONT	Downward continuation and gridding	
	gpcol1.job	Collocation job, blockwise solutions
	gpfit.job	Simple covariance estimation, use only as rough guide
GEOID	FFT and restore steps for geoid	
	bouguer.job	Job for making land Bouguer anomaly from downward continued, reduced gravity grid file "downrd.gri"
	n-zeta.job	Difference of geoid and quasigeoid, from DEM & Bouguer
	n_rtm.job	RTM geoid terrain effect by prism integration (slow task!)
	geoid.job	Composite geoid job, doing FFT, add terrain effect, add EGM, apply corrections for quasigeoid -> "ph_geoid.gri"
	geoip.job	Difference to GPS-levelling data (statistics and dif-file)
GPS-LEV	Geoid fit files	
	fitgeoid.job	Fitting of geoid to GPS-lev file with collocation. Always plot the following files to judge fit of "ph_geoid_fit":
	- fitgeoid_dif.dat:	point list with differences GPS-geoid
	- fitgeoid_dif.gri:	corrector surface for fitted geoid
Auxillary:	grid_int_ph.exe	User-friendly interpolation program
	se-asia.bna	Coastline file for "surfer" graphics

Note: to run GRAVSOFT on 64-bit Windows machines, check "job.bat" in GRAVSOFT directory for the following statement in line 2, it should read: jobb64 <%1.job (job <%1.job for Win32)

Forsberg, R. (2003). *Towards a cm-geoid for Malaysia*. Paper presented at the geoid computation workshop in Kuala Lumpur.

Forsberg R, C. C. T. (2008). Overview manual for the GRAVSOFT Geodetic Gravity Field Modelling Programs (Technical Report, 2nd ed.): DTU-Space.

Forsberg, R., D. Solheim & J. Kaminskis. (1996). *Geoid of the Nordic and Baltic area from gravimetry and satellite altimetry*. Paper presented at the Symposium on Gravity, Geoid and Marine Geodesy, Tokyo, 1996.

Forsberg, R., & Olesen, A. V. (2010). Airborne gravity field determination *Sciences of Geodesy-I* (pp. 83-104): Springer.

Forsberg, R., Strykowski, G., Iliffe, J., Ziebart, M., Cross, P., Tscherning, C. C., . . . Finch, O. (2002). OSGM02: A new geoid model of the British Isles. *Gravity and geoid*, 3.

Harlan, R. B. (1968). Eotvos corrections for airborne gravimetry. *Journal of Geophysical Research*, 73(14), 4675-4679.


<http://igscb.jpl.nasa.gov/>.

Kearsley, A. H. W. (1991). Evaluation of the geoid of the Philippines (Vol. 1): SAGRIC International.

Moritz, H. (1980). Advanced physical geodesy. *Advances in Planetary Geology*, 1.

Olesen, A. V. (2002). *Improved airborne scalar gravimetry for regional gravity field mapping and geoid determination*. Faculty of Science, University of Copenhagen.

PAHLEVI, A., PANGASTUTI, D., SOFIA, N., & KASENDA, A. (2015). *Determination of Gravimetric Geoid Model in Sulawesi-Indonesia*. Paper presented at the FIG Working Week.

Vanicek, P. (1991). Vertical datum and NAVD88. *Surveying and Land Information Systems*, 51(2), 83-86. 

Former ISRO chairman UR Rao dies

Eminent space scientist and former Indian Space Research Organisation (ISRO) chairman Udupi Ramachandra Rao passed away. He was 85.



He was suffering from age related ailments and breathed his last at his residence in the city. Rao is survived by his wife, a son and a daughter, ISRO officials said. Born in Adamaru area of Karnataka's Udupi district, Rao was involved in all ISRO missions till date in one capacity or the other. He is credited for contributions to the development of space technology in India and its extensive application to communications and remote sensing of natural resources.

Rao served as the chairman of ISRO for 10 years from 1984-1994. The eminent scientist, who was conferred a Padma Vibhushan earlier this year, was part of the Aryabhata and Mars Orbiter Missions. He was awarded the Padma Bhushan in 1976.

He also initiated the development of the Geo Stationary Launch Vehicle (GSLV) and the development of cryogenic technology in 1991. He has published over 350 scientific and technical papers covering cosmic rays, interplanetary physics, high energy astronomy, space applications, satellite and rocket technology and authored many books. Rao also became the first Indian space scientist to be inducted into the prestigious 'Satellite Hall of Fame' in Washington DC on March 19, 2013, and the 'IAF Hall of Fame' in Mexico's Guadalajara. www.hindustantimes.com

PCI Geomatics releases GXL 2017

PCI Geomatics has announced the release of GXL 2017, the latest version of its high-performance, scalable processing system for large-scale geo-image production. It continues to add to existing operational management, custom job-chaining, and fully automated production and reporting in secure, open, virtual and direct receiving stations (VRS/DRS), or cloud environments. pci geomatics.com

Odisha govt, India asks depts to provide data to OSRAC

The Odisha government, India has asked all its departments to use data being provided by the Odisha Space Application Center (ORSAC) in project monitoring and service delivery system.

The direction in this regard was issued by Chief Secretary A P Padhi while reviewing activities of the ORSAC here. He said the ORSAC had made the way for space based surveillance and monitoring through generation of remote sensing geo-coordinated data in the sectors like forest, agriculture, mining, land records, water resources, urban property assessment and natural resources. Padhi also directed the ORSAC to complete remote sensing based property tax assessment of Bhubaneswar and Puri municipal areas within three months.

During previous years ORSAC successfully developed the GPS tracking system of mineral carrying vehicles. As of now, 3,700 trucks are under its direct surveillance from the point of loading to the destination. Similarly, the Center developed remote sensing and GIS technology data base on actual irrigated area and cultivated area. The Center has showed the way for web based remote sensing crop cutting experiment in the year 2017, www.business-standard.com

Taiwan RS satellite launch scheduled

Taiwan's National Space Organization (NSPO) under the government-sponsored National Applied Research Laboratories (NARLabs) on July 19 transported FormoSat-5, a self-designed remote sensing satellite, to Vandenberg Air Force Base in California for launch on August 25, 2017 by US-based SpaceX on a commission basis using its Falcon 9 rocket, according to NSPO.

FormoSat-5 is the first satellite completely designed domestically, with NSPO directing the design through cooperation with the Instrument Technology Research Center under NARLabs, National Central University and private

Google's Waze launches navigation app for car dashboards

Waze is bringing its navigation and traffic monitoring app to more than 100 models of car as it expands its satnav software beyond smartphones.

The app will be available in cars that use Android Auto, Google's dashboard software, including models from BMW, Vauxhall, Renault, Ford and Volkswagen made in 2015 or after.

Waze, which is owned by Google and has 85 million users worldwide, offers route guidance using map data, travel times and traffic information. It can also advise drivers of incidents on the road and provide the latest fuel prices. Unlike traditional satnavs, which require large map downloads to operate offline, Waze updates in real time through smartphone data connections. It works with voice control and sends audio and visual traffic alerts. www.telegraph.co.uk

Automated cars won't be allowed in India, says Indian Minister

Indian government has denied the possibility of having self-driven cars on Indian roads because it doesn't want to promote any technology or policy that will make people jobless, said Nitin Gadkari, Minister for Road Transport and Highways.

"No driverless cars will be allowed in India. The government is not going to promote any technology or policy that will make people jobless," he said.

Gadkari said the country has a shortage of 2.2 million drivers and added that driving skills can provide employment to around five million people.

"Cab aggregators like Ola and Uber are making money by using our driving skills. If cab aggregators think they can make more money by introducing technology like driverless cars and render people unemployed, the government is not going to allow it," he said. ▽

enterprises mainly including Aerospace Industrial Development. With a weight of 450kg, FormoSat-5 is equipped with a domestically developed and made high-resolution optical remote sensing instrument which can capture images on a panchromatic spectral band at a resolution level of (12,000 pixels) two meters and four color spectral bands each at (6,000 pixels) four meters. In addition, FormoSat-5 carries an advanced ionosphere probe as a scientific payload to establish space weather models, observe changes in plasma turbulence, and study possible abnormal phenomena in the ionosphere before earthquakes. www.digitimes.com

India mulls aerial mapping for controlling floods

Appearing to have learnt lessons from the natural disasters that struck the State, including the nightmarish 2015 deluge in Chennai, the Tamil Nadu government has proposed to employ unmanned aerial vehicles (UAVs) to map water courses and river basins to chalk out a comprehensive flood control mechanism. The government has earmarked Rs7.01 crore for unmanned vehicle aerial photogrammetry for topographical mapping of waterbodies, particularly rivers and their courses, to find flood-causing factors and initiate rectification measures.

Explaining the project, K Satyagopal, Commissioner for Revenue Administration and Relief Commissioner, said that mapping would be done on the entire river basins to find out the points that caused floods during monsoon. "The unmanned vehicle aerial photogrammetry will help find out factors that trigger floods, to map drain canals to flush out water, link canals to divert water so that the damage could be minimised," he told Express. www.newindianexpress.com

Planet ground station caught in Canadian regulatory limbo

As Planet prepares to complete its initial constellation of remote sensing satellites, a ground station it built in northern Canada to communicate with those spacecraft remains offline because of

delays in receiving a government license there. The problem Planet has faced winning approval for its ground station, industry representatives argue, is a sign of outdated remote sensing regulations in Canada that could deter other companies from operating in the country.

Planet completed the ground station at Inuvik, in the Northwest Territories, early this year. The company said the latitude of the site, 68 degrees north, coupled with a fiber optic link to the town and a lack of radiofrequency interference in the area, made the location ideal as a major ground station to collect images from its constellation of cubesats. <http://spacenews.com>

NRSC in India establishes new outreach facility in Hyderabad

National Remote Sensing Centre (NRSC) established a new Outreach Facility at Jeedimetla Campus in Hyderabad to cater to the ever growing requirements of capacity building in Space-based applications. This facility caters to several activities like Training and Capacity Building, Information Kiosks, Content Generation, Outsourcing and Mass Communication, which could be conducted in parallel.

The facility, in its form, has large number of thin client systems connected to database servers and Bhuvan Geo-portal for massive content preparation. In addition, user has access to satellite data and various applications software for meeting specific requirements of NRSC.

Indian space scientist Yash Pal dies at 90

Indian space scientist and academician Yash Pal died in Noida, Uttar Pradesh. The 90-year-old had been unwell from a while, and breathed his last on Monday. Pal was well-known for his work on cosmic rays and his show on Doordarshan titled "Turning Point". He received the Padma Vibhushan in 2013 and various other awards throughout his career. △



China plans space-based, solar-powered telecom drones: Report

A research institute affiliated with China Aerospace Science and Industry Corp is developing the project "Feiyun," which means "flying cloud," the Global Times reported, citing another report in the Science and Technology Daily. The network will be based in "near space", it said, adding the system will be able to provide week-long emergency communications access and likely to go on trial this year.

The drones can fly as high as 20 kms above the ground for days - somewhat like a telecommunications satellite - and can undertake remote sensing and relay signals, the report quoted Ma Hongzhong, head of the institute, as saying.

Experts believe the technology can play an important role in aiding rescuers in the aftermath of natural disasters. However, they warned that the severe environment in "near space" - 20-100 kms above sea level - poses a challenge to the UAVs as the thin air inhibits the functioning of fuel-powered aircraft engines. <http://economictimes.indiatimes.com>

GeoCue Rolls out Kit for Equipping sUAS with PPK GNSS

GeoCue Group Inc., a North American supplier of kinematic LiDAR processing tools, has announced a new GNSS for users of DJI Phantom 4 Pro and Inspire 2 drones, as well as most drones using higher-end cameras. According to GeoCue, Loki, the company's new direct geopositioning system for small unmanned aircraft systems (sUAS), solves two fundamental problems: Positioning Accuracy and Camera Events. <https://unmanned-aerial.com>

NOAA and Ryka UAS Teaming Up on Wetland Restoration Project

Ryka UAS will soon begin working on a wetland restoration project with the National Oceanic and Atmospheric Administration (NOAA). With 28 populations of salmon and steelhead

listed as threatened or endangered due to habitat loss, Ryka UAS has been brought on to help evaluate the wetland restoration process through the use of drones and remote sensing. Other collaborators include the National Park Service (NPS) and Pacific Northwest National Laboratory (PNNL).

Each group will play a very important role in developing an effective restoration plan and executing it including approval from the NPS to fly within the Lewis and Clark National Park.

By equipping drones with Hyper-Spectral sensors, NOAA will be able to create catalogs of Pacific Northwest vegetation and invasive species that become harmful to wetland environments. This data will enable NOAA to analyze the status of the wetlands in an extremely detailed and comprehensive manner compared to traditional satellite and manned aircraft methods. The cataloged spectra collected from the imager will be formatted into a spectral library. <https://rykauas.com>

Drone unit 'historic step' for policing in UK

Devon and Cornwall and Dorset police forces began trialling the technology in November 2015 and the unit has now become fully established.

Five officers have been trained, with a further 40 aiming to complete their Civil Aviation Authority (CAA) accreditation in the next 12 months. There are currently six drones - equipped with a zoom camera and thermal imaging - in operation across the two forces. The drones take part in missing person searches, crime scene photography and respond to major road traffic collisions. They also help scour the forces' 600 miles of coastline, as well as woodlands, and help combat wildlife crime. www.newsandstar.co.uk

MicaSense Atlas is now integrated with Pix4D desktop software


Pix4D has announced the integration of its Pix4D desktop software with

MicaSense Atlas.

With this integration, Pix4D will offer MicaSense customers the power of desktop processing, as well as the flexibility of MicaSense Atlas.

With the new "Upload to Atlas" feature that will be available from August 8th, 2017, users can share the processed results with MicaSense Atlas directly from the Pix4D user interface.

senseFly announces Always On

senseFly has developed its Always On service package. Available as a bundle option alongside every new eBee Plus drone purchase, it provides operators with an advanced level of professional support and peace of mind. In the event of a drone hardware problem — whether the result of user error, a naturally occurring event or a technical issue — customers can simply contact their local senseFly representative to have their drone replaced for free within 48 hours, no questions asked*. 



**ITSNT**
TOULOUSE
www.itsnt.fr

ENAC
La référence aéronautique

NOV 14/17 International Technical Symposium
2017 on Navigation and Timing
Ecole Nationale de l'Aviation Civile in Toulouse, France





► 14-17 Nov 2017, ENAC, Toulouse, France
Join a unique international event

The ITSNT is evolving: check out the changes on our website

Seize the opportunity to exchange with **world recognized speakers** on hot technical topics such as navigation trends in GNSS-denied environments, UAV navigation, GNSS integrity and resilience, space applications of GNSS and much more.

Visit our **exhibitors**

Don't miss our **tutorials for professionnals**

Register now on www.itsnt.fr

Pôle multimédia CNES - 2017-324

GOLD SPONSOR



SILVER SPONSORS



BRONZE SPONSOR



Coastal Protection in Thailand by SuperSurv 10

Supergeo has announced that the cutting-edge mobile GIS app- SuperSurv 10 has been selected by a government agency that is in charge of protecting marine and coastal resources in Thailand for spatial data collection. The core mission of this department is to conserve and restore the precious flora and fauna resided in the marine and coastal ecosystem. For the government authority of environmental protection and ecological monitoring, one of the most important tasks is to patrol the conservation areas and record the species of flora and fauna regularly. To achieve this goal, field workers should bring handheld GNSS devices to the field, activate mobile GIS software to check current position, and record the attributes of specified animals or plants. Based on Android OS, SuperSurv 10 is mobile GIS equipped with both basic and advanced GIS features that can significantly assist spatial data collection. www.supergeotek.com

Palestine will wait for new GIS map

A map of the village at the county courthouse hasn't been updated since 1984, and the East Palestine Area Chamber of Commerce was hoping to change that. The map was done by the chamber and provided to the courthouse for public use. Chamber treasurer Bonnie Davis, who also works at the courthouse, said that she looked into whether it would be possible to make a new, updated map of East Palestine, but learned it would cost a few thousand dollars.

"We would have to hire someone to do that," she told the chamber at its recent meeting.

Chamber member and past director Tim Weigle said that a new map likely wouldn't be needed, since a new countywide GIS map will provide the information. Weigle is also on the board of county commissioners, which back in May approved a request from Auditor Nancy Milliken to hire Ohio University for development of a GIS. www.morningjournalnews.com

Drone-based GIS mapping of Panaji on cards under Smart City Mission

Imagine Panaji Smart City Development (IPSCD) limited, India has decided to take up GIS mapping of the capital to improve municipal tax collection and to identify municipal tax defaulters. IPSCD, the special purpose vehicle formed to implement the Smart City Mission has announced that it would create a GIS-based masterplan for the capital. GIS mapping will also be used to identify utility services, which will come in handy while planning the city and giving permissions for digging. All the data collected will be stored on a digital database. <http://timesofindia.indiatimes.com>

OS releases open dataset and free map of Britain's greenspaces

To make it easier for people to locate and access greenspaces, the UK government has released a new database and interactive digital map that identifies accessible recreational and leisure greenspace in Great Britain. Delivered by Ordnance Survey (OS), the map is available for free and contains the data from OS and other sources. This is achieved by OS Maps' popular leisure mapping app and online service.

This comprehensive map of Great Britain's greenspaces is also available as an open dataset, called OS Open Greenspace, for communities, businesses and developers to create products and services that will encourage healthier and greener lifestyles.

Since the greenspace map was reaffirmed as a commitment in 2015, OS has worked in collaboration with a large number of non-government organizations and government partners to compile the OS Open Greenspace dataset and digital map. www.osmaps.uk/greenspace.

Pune India completes GIS mapping of 2.5 lakh properties

The Pune Municipal Corporation (PMC), India has completed almost 33% of the

'geo' enabled property tax survey to automate its entire property tax assessment function. PMC is expecting to complete the remaining work in the next six months.

Property tax department head, Suhas Mapari, said that there are around 8 lakh properties in the city and the municipal corporation is doing its GIS base mapping to increase its revenue and to calibrate the identified unassessed properties.

The PMC is undertaking a door to door survey for doing the GIS mapping and then feeds the necessary information into the software. It is a tiresome task, but once the project would be complete, it would be very helpful for the civic body as all the information would be available at one click. www.hindustantimes.com

Solutions to Transform Building and Construction Industry

ISYX Technologies, a fast-growing business innovation consulting company in the Middle East and Africa, successfully held a joint workshop with Microsoft on the challenges faced by the construction and building materials industry. The event focused on how specific solutions provided by ISYX Technologies using Microsoft Dynamics 365 can improve the productivity of the industry players on various projects.

The key objective of the workshop was how to focus on the improvement of specific project parameters like sales automation, supply chain and delivery, material estimation, project P&L management, dashboard, KPI's per project, resource allocation per project, service maintenance, amongst others.

D365 is completely project-centric and is a work-breakdown structure, driven solution. It covers actual versus budget variance analysis, material variance, labour variance, cash flow analysis, EVA analysis, projected cash flow over six-month period, project portfolio analysis, amongst others. It provides coverage for every process of a project based organization. <http://mid-east.info>

DFS launches Precision Navigation

A new precision navigation procedure, RNP-1 (Required Navigation Performance), has been launched at Frankfurt International Airport, according to German air navigation service provider (ANSP) DFS. With RNP-1 and Radius-to-fix, they are increasing their precision navigation in air traffic to a new quality level, which has not been achieved in Germany.

Pilots using this method, in a high degree of precision, are passing through a circular path, which is defined by the air traffic control on the basis of a fixed radius, starting from a fixed point. This allows aircraft to maintain their predefined ideal line in a curved flight with a continuously equal distance from the reference point. This results in positive effects on the noise effects for the inhabitants of the region. The extent to which this effect will be can not yet be estimated with sufficient certainty, DFS says.

Simulations have shown that RNP-1 and Radius-to-fix aircraft allow aircraft to travel more precisely, even under difficult wind and weather conditions. DFS is now testing this new process for six months on the existing conventional take-off route, the so-called “Südumflug”, on its accuracy. In order to be able to fly any RF leg, aircraft must be equipped with modern and RNP-1-approved satellite navigation technology. www.aviationtoday.com

Australia's first GPS infrastructure officially in space

Australia officially has its first GPS infrastructure in space, according to the nation's Minister for Defence Industry Christopher Pyne.

A four-kilogram, U.S.-developed Biarri-Point cubesat was launched as part of the QB50 constellation in April 2017 towards the International Space Station (ISS), alongside three other Australian research cubesats.

Biarri-Point was deployed in May from the ISS into its own low Earth orbit (LEO), carrying the Namaru GPS technology — the first fully Australian and New Zealand GPS payload for a cube-satellite. The Biarri project is a four-nation defense-related project involving Australia, the U.S., the UK and Canada. The Biarri-Point miniature satellite is the first of four Biarri cubesats to be deployed in the effort to learn more about cubesat formation flying and the drag and lift forces affecting signals from cubesats. The expectation is to inform future applications of satellite positioning with GNSS, including for future high precision satellite-based augmentation system (SBAS) and precise point positioning (PPP) capabilities, as well possible defense applications.

Biarri-Point is equipped with a L1 signal GPS receiver designed to measure the precise relative position of the Cubesats in its LEO. The spacecraft is also fitted with corner reflectors, thereby allowing the satellites to also be located using satellite laser ranging (SLR).

Inertial Navigation System

NEW



0.1° Roll & Pitch
0.2° Heading
2 cm RTK



Ellipse-D Dual GNSS/INS

- » Immune to magnetic disturbances
- » L1/L2 GNSS receiver

- » Accurate heading even under low dynamics
- » Post-processing

Glomass update

Russia, China to set up pilot zone to test national navigation systems

Russia and China are set to establish a pilot zone to test the Russian GLONASS and Chinese BeiDou satellite navigation systems on passenger and freight transportation routes going through Kraskino - Hunchun and Poltavka - Dongning checkpoints on the border in Russia's Primorsky Territory, the Russian Transport Ministry said.

The issue was discussed during a meeting of a bilateral working group on road transport and roads. The sides also discussed the possibility of opening a new international route going through Russia's Novosibirsk, Irkutsk and Zabaykalsk cities and Chinese cities of Manzhouli, Yingkou and Dalian, according to the statement. <https://sputniknews.com>

Restrictions on buying foreign equipment for GLONASS

The Russian government has listed equipment for the GLONASS system as a foreign-made equipment that is restricted access for purchasing for state and municipal needs, the Cabinet of Ministers posted the report with Prime Minister Dmitry Medvedev's signature on its web site on Tuesday.

"Under the signed order, the GLONASS equipment, electronic warning system, electronic equipment for security and traffic control were added to this list due to the fact that micro schemes and modules for the GLONASS navigation equipment had been developed and studied in Russia, as well as the production of lighting facilities and its parts that compete with foreign analogs in their specifications," the explanatory note to the document says.

The note says that the taken decision is aimed at increasing competitiveness of Russian products, reduction of the domestic market dependency on imported goods in the spheres of

security and traffic control, as well as development of microelectronic products. <http://tass.com/economy/955727>

GLONASS proposed as early warning tsunami detection system

Signals sent by the GLONASS and GPS satellites have been suggested to be used for radar location of large waves in oceans, a report of the Conference on Current Aspects of Remote Sensing of Earth from Space says.

"The appearance of numerous navigation satellites made it viable to study the possible use of reflected navigation signals for radar location of the water and Earth's surfaces," the report says.

For this, it was proposed to look into the possible launch of a space object with a signal receiver for navigation systems and a multi-beam antenna into the near-Earth orbit (400 km above the Earth), so that signals reflected from the Earth's surface could be received from ten or more navigation satellites. In this case, one satellite will be able to sense the whole Earth's surface in twenty-four hours. This technology may be used to measure movement on the Earth's surface, sea surface parameters, including unsafe sea monitoring and tsunami early warning, as well as the speed and direction of the wind over the sea surface, ice thickness in polar regions and monitoring object movements on the Earth's surface. The report reiterates that the first experiments with bistatic radiolocation (in which a transmission unit and a receiver are located far from each other and move at different speeds regarding the studied object) of the Earth from space were carried out in Russia in 1989-1998 with the use of the Mir space station. Geostationary satellites radiated radio waves to the Earth, and the Mir station received the reflected signal. The outcome analysis showed the efficiency and potential of the suggested method of bistatic radiolocation. <http://tass.com/science/956089>


Consortium Records Scintillation on Galileo Signals in Antarctica

At the end of last year, the DemoGRAPE consortium observed, for the first time ever, ionospheric scintillations on Galileo signals in Antarctica, using Septentrio's PolaRx5S GNSS reference receiver. DemoGRAPE investigates improvement of high-precision satellite positioning with a view to developing scientific and technological applications in Antarctica.

At higher latitudes, GNSS signal degradation due to ionospheric activity is more pronounced. The more precise phase-based positioning modes are particularly vulnerable to ionosphere disturbance such as scintillations. Elevated ionospheric activity can cause a loss of precise-positioning mode or, in more extreme cases, a total loss of signal lock

DoT makes GPS compulsory for handsets

Department of Telecom (DoT), India has made it compulsory for all the mobile phones to have GPS since January 1, 2018. Apart from GPS, it is also mandatory for phones to have a physical panic button on every device. The move comes on the back of security concerns, especially involving women, elders and children as mandating GPS would enable phones to have better location accuracy while under surveillance.

Interestingly, Telecom Regulatory Authority of India (TRAI) in October 2015 had pushed device manufacturers to make GPS mandatory in handsets. However, DoT rejected the proposal citing lack of proper studies and impact of such a decision. Device manufacturers have urged the government against DoT's decision as they suggest the move will increase the cost of feature devices by at least 30 percent. The device makers are suggesting an alternate option of implementing triangulation of telecom towers method to locate devices. The plus point with this method is that it can work even with no data connection. However, DoT argues that triangulation method is inaccurate, unlike GPS. www.moneycontrol.com 

Trimble introduces new android application

Trimble has introduced Trimble® Penmap® for Android™, a cloud-connected application for field surveying and high-accuracy GIS data collection that works on mobile handhelds, smartphones and tablets. Trimble Penmap for Android focuses on core survey and mapping tasks such as cadastral and boundary surveys, establishing local control, stake-outs, quality checks and asset management for utilities. It provides both professional surveyors and field workers with an intuitive, easy-to-use map-based interface to manage features and attributes for high-accuracy GIS and complete survey documentation. For example, the application is ideal for use in the energy distribution industry for locating infrastructure and recording critical information on encroachments, clearways and existing monuments. The application runs on a variety of Android devices, including the rugged Trimble TDC100 handheld, and supports full-featured Trimble GNSS receivers such as the Trimble R10, R8s and R2 receivers.

It is optimized to integrate with the new Trimble Catalyst™ service, a software-defined GNSS receiver that connects to the small, inexpensive plug-and-play DA1 antenna, and allows surveyors to choose an accuracy level from meter to centimeters to suit their application needs. www.trimble.com

DAT/EM Systems international updates landscape software

DAT/EM® Systems International has released version 7.4 of its software suite, including significant updates to LandScape, a 3D stereo point cloud editing and visualization tool. In LandScape version 7.4, operators can expect to load points in half the time as previous releases, utilize more filters and tools to explore their point clouds, and have the option to purchase the new Point Cloud VR to view their point cloud in virtual reality (VR). Photogrammetric, engineering and GIS professionals use LandScape to quickly view and modify enormous

terrain point clouds from sources such as aerial LiDAR, structure from motion (SfM) and unmanned aerial systems (UAS). www.datem.com/landscape.

Solution for A-BeiDou LBS by Rohde & Schwarz and MediaTek

Rohde & Schwarz and MediaTek have successfully completed the verification of location based services (LBS) in the U-plane and C-plane for A BeiDou, the new GNSS satellite positioning system from China. The R&S TS-LBS test solution allows mobile manufacturers, chipset manufacturers, test houses and network operators to verify chipsets and mobile devices in order to obtain permission to operate them in a particular network.

The R&S TS LBS from Rohde & Schwarz is a test system for testing GNSS and network-based LBS. It consists of an R&S CMW500 as the base station simulator and an R&S SMBV100A GNSS simulator. The R&S CMW500 provides assistance data to the DUT and the R&S SMBV100A simulates the BeiDou satellites. The R&S TS-LBS test system can be used to obtain GCF and PTCRB certification as well as network operator specific certification for chip sets and mobile devices. www.rohde-schwarz.com

NovAtel Technology, AutonomouStuff Featured in Baidu Apollo Project

Baidu has announced NovAtel's partner, AutonomouStuff, as a member of their Autonomous Driving ecosystem — Project Apollo.

Project Apollo has been initiated to provide an open, comprehensive and reliable software platform for Baidu's partners in the automotive and autonomous driving industries. Partners can use the Apollo open software platform together with the reference hardware platform to accelerate development of their customized autonomous vehicle solutions. Based on their extensive experience in autonomous system development, it will provide the "Apollo Kit" to Baidu Apollo partners. The Apollo Kit includes the vehicle – a Lincoln

MKZ with by-wire kit installed – and all hardware, software and services required for an Apollo partner to quickly begin developing their autonomous vehicle. NovAtel SPAN GNSS/INS products will provide position, orientation and time as a critical component of the Apollo Kit.

Harxon releases rover radio for RTK surveying and GNSS positioning

Harxon has introduced an advanced, high-speed, Bluetooth-enabled wireless rover radio. The HX-DU1603D. The HX-DU1603D is a lightweight, ruggedized UHF receiver designed for data communications between 410 MHz and 470 MHz in either 12.5 KHz or 25 KHz channels, which can be widely used in GNSS/RTK surveying and GNSS precise positioning fields. It is equipped with a Bluetooth transceiver for wireless communications with external devices. It features a 6800 mAh rechargeable internal battery and configurable transmit power between 0.5W and 2W. Its IP67 waterproof capability allows long operating hours outdoors, the company said.

Data Collecting Program for Mobile GNSS Field Data Set taking Place in Japan

Lighthouse Technology and Consulting Co., Ltd is proceeding with a program to collect precise GNSS data on major highways in Japan. The data is an inevitable "must use" tool for high precision positioning systems used in automated driving vehicles. While the major part of autonomous driving systems consists of sensors and image recognition technologies, satellite positioning is also a key element used for complementing the precise current position.

There are obstacles to overcome with automated driving on public streets, and the competition among companies to develop solutions is accelerating due to recent technological advancements in sensors, image recognition, and artificial intelligence. In addition, Japan's Quasi-Zenith Satellite System (QZSS) has brought attention to developments in centimeters leveled high precision

positioning. When dealing with satellite positioning technology for automated driving systems, it is inevitable to have a variety of high precision field data at the point of development, testing, and fine tuning prior to the driving test of the vehicles, and to have the reference position data at the point of evaluation.

Orolia's McMurdo wins U.S. Search and Rescue Technology Awards

Government Security News has named McMurdo, an Orolia brand, the winner of two national search and rescue technology awards in its annual Airport, Seaport, Border Security Awards Program. McMurdo won Best Search and Rescue and Best Man Overboard Tracking in the Maritime/Port Security/Underwater Vehicles and Communication Systems categories, respectively.

McMurdo delivered a series of industry firsts to revolutionize the way search and rescue missions are conducted today. In 2001, McMurdo was the first to deliver individual emergency distress devices with its Personal Locator Beacon (PLB). The U.S. Coast Guard has recently selected McMurdo to provide up to 16,000 PLBs to enhance crew safety. In 2011, McMurdo delivered the first Man Over Board (MOB) devices. Today, their MOBs provide extremely accurate location information and transmit automatically when a life jacket inflates, according to the company.

Orolia holds a pioneering role in search and rescue (SAR) technology. The company's position as the top provider of Medium Earth Orbiting Search and Rescue (MEOSAR) satellite-aided technology has reduced the time required to detect emergency signals from hours to near instantaneous detection.

Sierra Wireless offers LPWA module with GNSS

Sierra Wireless, a provider of fully integrated device-to-cloud solutions for the Internet of Things (IoT), is offering global, dual-mode low-power wide-area (LPWA) cellular modules. The AirPrime WP77 smart wireless modules

simplify LPWA deployments for customers developing products that need to connect to multiple networks where different LPWA technologies are supported.

The WP series simplifies development for secure telematics and gateway applications, providing a dedicated application CPU core running the Linux-based open source Legato application framework.

Tersus launches the NeoRTK system to enhance surveying

Tersus GNSS Inc. has launched the NeoRTK System with multi technology integrated for surveyors. The system is described as a new generation system by the company and is applied with multi-constellation and a multi-frequency GNSS engine and various communication protocols which aim at providing high performance and stable signal reception to meet surveyors' demands. Featuring a high-end GNSS antenna inside, the NeoRTK can speed up the Time to First Fix (TTFF) and improve the capability of anti-jamming.

The 16G internal storage and up to 32G external SD card along with the built-in large capacity battery for 10-hour field work can assist surveyors' productivity in their daily practice. The radio module in the package makes long distance operation more convenient.

Esri Expands Its World Geocoding Service Capability

Esri, have announced the release of significant enhancements to the World Geocoding service for the company's ArcGIS platform. This update to the World Geocoding service gives users access to 25 additional countries, including Cuba, Bangladesh, and Libya, where street addresses can be located.

World Geocoding empowers users to easily convert addresses into locations—and vice versa—on a map. These new enhancements include improvements such as refined address matching using the latest authoritative datasets, and easier

identification of real locations. For the complex problem of intersection matching, the service has been improved to recognize more diverse types of intersections on a visual map showing features that don't physically meet, like overpasses above other roads, or streets that are connected by roundabouts. Coordinates can also be matched to points of interest, postal regions, administrative areas, and countries for enhanced reverse geocoding.

SXblue Introduces Its Ultimate Survey Grade GNSS Receiver

SXblue Platinum is the latest model in the SXblue series. This high accuracy GNSS receiver is compatible with iOS, Windows and Android Bluetooth, and provides real-time professional-grade positioning information.

Powered by its 394 channels, the SXblue Platinum uses all-in-view constellations (GPS, GLONASS, Galileo, BeiDou and QZSS) with triple frequency, and provides the ability to use global or local coverage for corrections (SBAS, L-Band and RTK). The receiver is field-upgradable which means that these options can be remotely activated at your convenience.

MicroSurvey CAD 2017 released

MicroSurvey Software Inc. is proud to announce the release of MicroSurvey CAD 2017 with powerful new and enhanced capabilities, streamlined workflows, and important bug fixes that continue to make MicroSurvey CAD the absolute best choice for land surveying and civil engineering professionals worldwide.

MicroSurvey CAD provides users with an intuitive interface on a complete survey drafting toolkit, including COGO, DTM, traversing, adjustments, volumes, contouring and more. It is perpetually licensed and is powered by IntelliCAD® which is compatible with AutoCAD® drawing files. With five available feature levels – Basic, Standard, Premium, Ultimate and Studio – it gives users the choice between several tiers of features to ensure they are getting precisely the tools they need.

Mapping the World with Advanced LiDAR

Carbomap, an environmental survey company, in collaboration with high performance LiDAR manufacturer RIEGL, UAVE and The University of Edinburgh have announced the first successful demonstration flight of a RIEGL VUX-1LR survey-grade waveform laser scanner on a fixed wing, long range unmanned aerial vehicle (UAV). This is likely the first time that such a high-performance scanner has ever flown on a fixed wing UAV with such an advanced specification for long duration (8 hrs) and long range (1,000 km).

With centimetre-scale 3-dimensional accuracy, this breakthrough development will greatly increase the worldwide accessibility to high quality laser scanning (known as LiDAR). However, obtaining such high quality 3D data can be very expensive to obtain using conventional airborne surveys. It is difficult to process without specialised software, and as a


consequence, it is rarely available in most developing nations. By bringing such instruments together into a single UAV system (named Forest-Lux or F-Lux, for short), together with its own solution-focused software, it is now possible to get a system that can be a local asset, under local stakeholder control, and be operated at an affordable price in any country in the world.

Leica Geosystems' new 3D imaging laser scanner now available in Europe

Leica Geosystems, have announced its award-winning BLK360 miniaturised 3D imaging laser scanner is now available for reservation within Europe, for delivery in summer. The laser scanner simplifies the collection of as-built reality capture data for work in architecture, design, construction and engineering among other vertical markets.

Users simply place the lightweight BLK360 on a level surface or tripod and, with the push of a single button, it

captures 360° HDR spherical imagery and takes a 360,000 point per second laser scan. Getting measurements right the first time, the BLK360 features $\pm 4\text{mm}$ accuracy at 10 metres and an overall 0.6 - 60 metre range. Within three minutes, the spherical image and laser scan is completed and ready to view in the Autodesk ReCap Pro for mobile app, which runs on an iPad Pro. From there, users can take measurements, add markup and annotations or share onsite data with their colleagues back in the office.

"The BLK360 brings together exclusive technologies to deliver outstanding performance, all while simplifying the process of 3D image scanning and reality capture through the touch of a single button," said Burkhard Boeckem, CTO, Leica Geosystems. "This has enabled us to create new opportunities for scanning experts and introduce entirely new audiences to laser scanning while uncovering possibilities that were previously unimaginable." 

LINERTEC

Linertec, your Benefit in Surveying and Construction

The Linertec Precision Instruments are designed and developed in Japan. They are the result of our long-established expertise in Surveying and Construction.

LGP-300 Series
WinCE Reflectorless
Total Station

LTS-200 Series
Reflectorless
Total Station

LTH-02/05
Electronic
Theodolite

LGN-100N/T
Positioning
System

A-200 Series
Automatic
Level



SUBSCRIPTION FORM

YES! I want my **Coordinates**

I would like to subscribe for (tick one)

☐ 1 year ☐ 2 years ☐ 3 years

12 issues 24 issues 36 issues

Rs.1800/US\$100 Rs.3000/US\$170 Rs.4300/US\$240

**SUPER
saver**

First name

Last name

Designation

Organization

Address

.....

City Pincode

State Country

Phone

Fax

Email

I enclose cheque no.

drawn on

date towards subscription

charges for Coordinates magazine

in favour of 'Coordinates Media Pvt. Ltd.'

Sign Date

Mail this form with payment to:

Coordinates

A 002, Mansara Apartments

C 9, Vasundhara Enclave

Delhi 110 096, India.

If you'd like an invoice before sending your

payment, you may either send us this completed

subscription form or send us a request for

an invoice at iwant@mycoordinates.org

50 | **Coordinates** August 2017

MARK YOUR CALENDAR

September 2017

INSPIRE 2017

4 - 5 September, Kehl Germany
6 - 8 September, Strasbourg France
<http://inspire.ec.europa.eu>

Interdrone 2017

6 - 8 September
Las Vegas, USA
www.interdrone.com

ESA-JRC Summer School on GNSS 2017

4 - 15 September
Svalbard-Spitsbergen, Norway
www.esa-jrc-summer-school.org

56th Photogrammetric Week '17

11-15 September
Stuttgart, Germany
www.ifp.uni-stuttgart.de/phowo

ION GNSS+ 2017

25 - 29 September
Portland, USA
www.ion.org

Intergeo 2017

26 - 28 September
Berlin, Germany
www.intergeo.de

October 2017

GIS Congress-2017

2 - 3 October
Vienna, Austria
<http://gis-remotesensing>

The 9th Multi-GNSS Asia (MGA) Conference

9 - 11 October
Jakarta, Indonesia
<http://www.multignss.asia>

Year in Infrastructure Conference

10 - 12 October
Singapore
<https://www.bentley.com/en/yii/home>

GeoAdvances 2017

14-15 October
Safranbolu, Turkey
<http://geoadvances.org>

INGEO2017

18 - 20 October
Lisbon, Portugal
<http://ingeo2017.lnec.pt/index.html>

ACRS 2017

23 - 27 October
New Delhi, India
www.acrs2017.org

6th International Colloquium – Scientific and Fundamental Aspects of GNSS/Galileo

25 - 27 October
Valencia, Spain
<http://esaconferencebureau.com/2017-events/17a08/introduction>

3D Australia Conference 2017

26 - 27 October
Melbourne, Australia
<http://3dgeoinfo2017.com>

ITS World Congress 2017

29 October - 2 November 2017
Palais des congrès de Montréal, Quebec
itsworldcongress2017.org

November 2017

37th INCA INTERNATIONAL CONGRESS

1 - 3 November
Dehradun, India
<http://incaindia.org>

PECORA 20- 2017

14 - 16 November
South Dakota, USA
<https://www.asprs.org>

International Technical Symposium on Navigation and Timing (ITSNT)

14 - 17 November
Toulouse, France
<http://www.itsnt.fr>

Commercial UAV Show and GeoConnect Show 2017

15 - 16 November
London, UK
<http://www.terrapinn.com>

INC 2017

27 - 30 November 2017
Brighton, UK
<http://www.internationalnavigationconference.org.uk>

December 2017

International Symposium on GNSS (ISGNSS 2017)

10-13 December
Hong Kong
www.lsgu.polyu.edu.hk

February 2018

GMA: Geodesy, Mine Survey and Aerial Topography

15 - 16 February
Moscow Novotel Center, Russia
<http://www.con-fig.com/?lang=eng>

March 2018

Munich Satellite Navigation Summit

5 - 7 March
Munich Germany
www.munich-satellite-navigation-summit.org

April 2018

The 7th Digital Earth Summit 2018

17 - 19 April
El Jadida, Morocco
<http://www.desummit2018.org/>

Aiming at the future together!

PENTAX



D-600

Precise Aerial Imaging System

6 Rotor Multicopter with Autopilot



R-1500N

Reflectorless Total Station

Total surveying solution

W-1500N

Windows CE Total Station

A truly integrated system



G6 Ti|Ni G5 Tw|Nw|Tt|Nt G2100 T|N

GNSS Receivers

Precision Satellite Surveying with wireless communications



S-3180V

Scanning System

3D laser measurement system

TI Asahi Co., Ltd.

International Sales Department
4-3-4 Ueno Iwatsuki-Ku, Saitama-Shi
Saitama, 339-0073 Japan

Tel.: +81-48-793-0118
Fax: +81-48-793-0128
E-mail: International@tiasahi.com

www.pentaxsurveying.com/en/

Authorized Distributor in India

Lawrence & Mayo Pvt. Ltd.
274, Dr. Dadabhai Naoroji Rd.
Mumbai 400 001 India

Tel.: +91 22 22 07 7440
Fax: +91 22 22 07 0048
E-mail: instmum@lawrenceandmayo.co.in

www.lawrenceandmayo.co.in

The Only Limitation is Yours



SP90m GNSS Receiver

Have you ever thought about being able to work anywhere, anytime? Now, there's no limit to field work.

The Spectra Precision SP90m is a powerful, highly versatile, ultra-rugged and reliable GNSS positioning solution for a wide variety of applications in real-time and post-processing.

It also comes with a variety of integrated communications options, such as Bluetooth, WiFi, UHF radio, cellular modem and two MSS L-band channels to receive Trimble RTX correction services.

Versatile, Rugged and Reliable

- Most versatile, modular receiver design
- Ultra-rugged design
- Patented Z-Blade technology
- 480-channel ASIC
- Dual GNSS antenna inputs

AMERICAS: +1-720-587-4700 or 888-477-7516 (Toll Free in USA)

EUROPE, MIDDLE EAST AND AFRICA: +33-(0)2-28-09-38-00

ASIA-PACIFIC: +65-6348-2212

To find out more visit www.spectraprecision.com



© 2017, Trimble Inc. All rights reserved. Spectra Precision and the Spectra Precision logo are trademarks of Trimble Inc or its subsidiaries. All other trademarks are the property of their respective owners. (2017/07)